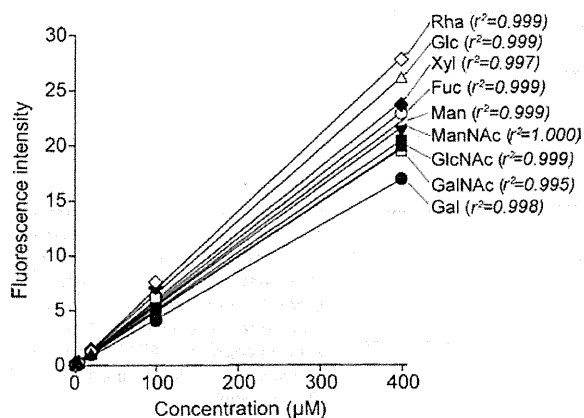


**Scheme 2.** Enzymatic conversion of sialic acids in glycoproteins to mannosamine derivatives.



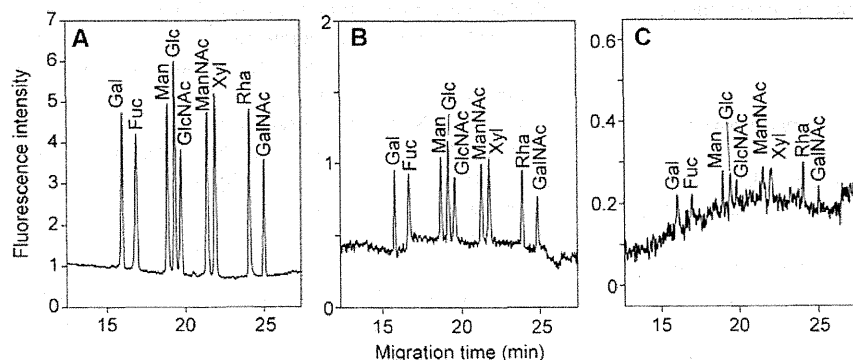
**Figure 2.** Calibration plots for quantitation of nine saccharides as AMC derivatives.

recovery of monosaccharides vary depending on the type of monosaccharides [20]. Therefore, we used different conditions for neutral aldoses, hexosamines, and sialic acids. Two molar TFA was chosen for hydrolysis of neutral aldoses, including Fuc, Gal, and Man, while 4 M hydrochloric acid was used for the release of hexosamines. Hydrolysis was performed at 100°C for 6 h. In contrast sialic acids are easily decomposed in strong acids so we chose enzymatic release and the generated neuraminic acids were further converted to *N*-acetyl- or *N*-glycolylmannosamine derivatives by the action of aldolase (*N*-acetylneuraminic acid pyruvate-lyase, EC 4.1.3.3), as shown in Scheme 2 [15]. Therefore, the contents of both types of neuraminic acid could be estimated from the peak areas of corresponding mannosamine derivatives, appearing at 17.5 and 18.5 min, respectively.

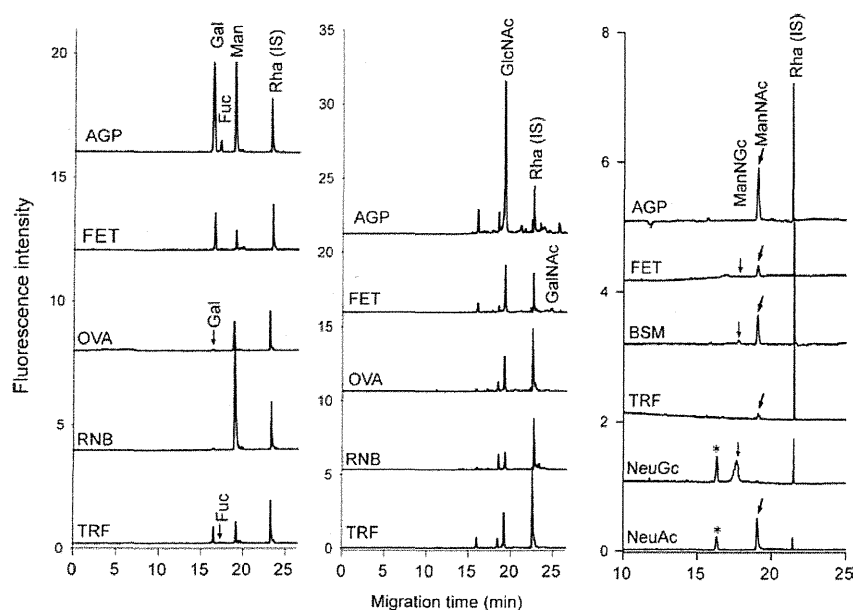
Figure 4 indicates the results of monosaccharide analysis of several glycoprotein samples. Rha was chosen as a common IS for the analysis. Acid glycoprotein, fetuin, ovalbumin,

ribonuclease B, and transferrin were chosen as common glycoproteins, and BSM was used for sialic acid analysis because mucin contains high concentrations of NeuAc and NeuGc. Carbohydrate chains of acid glycoprotein and transferrin are composed of complex oligosaccharides, whose chains consist of GlcNAc, Man, Gal, Fuc, and NeuAc [21, 22]. Electropherograms clearly indicated the presence of these monosaccharides. The fucose content of transferrin is low but the electropherogram clearly indicated the presence of Fuc in the hydrolysates of transferrin. Fetuin contains both *N*- and *O*-linked glycans [23–25]. Therefore, the oligosaccharide chains are composed of GlcNAc, GalNAc, Man, Gal, and neuraminic acids. These monosaccharides appeared in the electropherograms. Moreover, a small peak of *N*-glycolylmannosamine indicates the presence of NeuGc in this glycoprotein, at a level one order lower than that of NeuAc. Ovalbumin comprises high-mannose type and a series of hybrid-type glycans, which implies the presence of GlcNAc, Man, and a small quantity of Gal [26–28]. RNB comprises a series of high-mannose type oligosaccharides [29]. Therefore, hydrolysates include only Man and GlcNAc. These monosaccharides appeared in electropherograms.

Based on the peak area of each sample relative to IS, the monosaccharide contents were estimated and are summarized in Table 1. The results were compared to those of previously reported data [15, 30]. The accuracy of the present method involving the hydrolysis process could not be fully evaluated by comparison with previous data as contents of fucose in acid glycoprotein, Man in fetuin, and GlcNAc and neuraminic acids in transferrin were apparently lower than the reported values. In contrast, Man in ribonuclease and hexosamines in fetuin were at higher levels than previously reported. The sialic acid contents of BSM were three times higher than those of reported values, which should be due to difference in commercial preparation. We believe the removal of the purification step for derivatives could enhance the



**Figure 3.** CE analysis of nine saccharides at concentrations of 4 µM (A), 0.4 µM (B), and 0.04 µM (C). Analytical conditions were the same as those used for Fig. 1B.



**Figure 4.** Analysis of component monosaccharides in hydrolysates of various glycoproteins. Analytical conditions were the same as those used for Fig. 1B. ManNGc and ManNAc were derived from NeuGc and NeuAc, respectively. AGPa =  $\alpha_1$ -acid glycoprotein, FET = fetuin, OVA = ovalbumin, RNB = ribonuclease B, TRF = transferrin.

**Table 1.** Estimated content (%) of monosaccharides in various glycoprotein specimens

Glycoprotein	Man <sup>a)</sup>	Gal <sup>a)</sup>	GlcNAc <sup>a)</sup>	GalNAc <sup>a)</sup>	NeuAc <sup>b)</sup>	NeuGc <sup>b)</sup>	Fuc <sup>a)</sup>
$\alpha_1$ -Acid glycoprotein (human)	5.80	8.99	13.88	N.D.	10.02	N.D.	0.47
	5.50	7.60	13.20	N.D.	10.90	N.D.	0.70
Fetuin (bovine)	1.60	3.15	4.26	1.30	6.28	0.68	0.04
	2.45	3.49	2.62	0.54	4.62	–	0.03
Transferrin (human)	1.15	0.76	1.27	N.D.	0.91	N.D.	0.07
	1.08	1.00	1.79	0.05	1.40	N.D.	
Submaxillary mucin (bovine)	–	–	–	–	5.80	4.59	–
	–	–	–	–	1.69	1.25	
Ovalbumin (hen)	2.47	0.11	1.63	N.D.	N.D.	N.D.	N.D.
	2.80	0.12	0.28	N.D.	N.D.	N.D.	N.D.
Ribonuclease B (bovine)	4.63	N.D.	1.09	N.D.	N.D.	N.D.	N.D.
	2.20	N.D.	0.91	N.D.	N.D.	N.D.	N.D.

Values appearing on the lower line for each glycoprotein indicate reference values. N.D.: not detected; –: not determined.

a) Ref. [30].

b) Ref. [15].

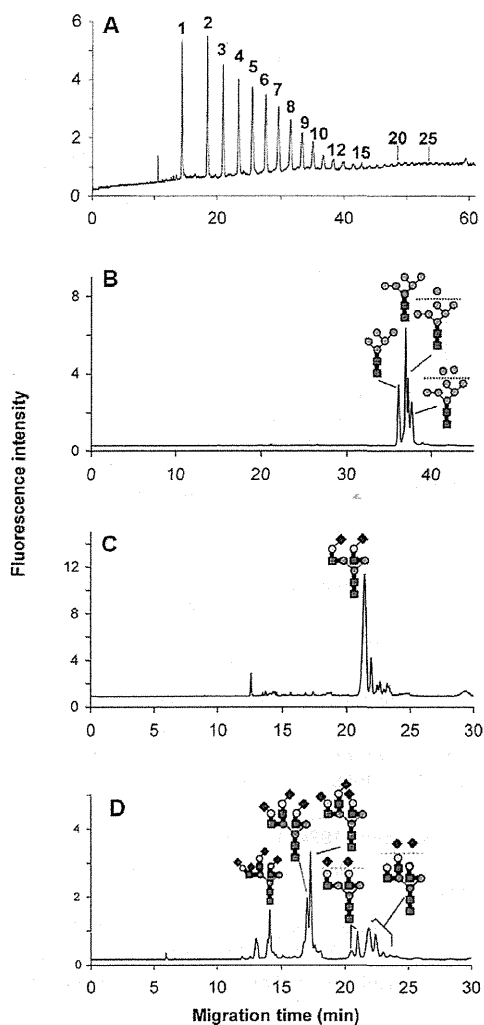
reliability of quantitation for saccharides in glycoconjugate samples. Our data may therefore be more reliable than that from previously reported methods and, moreover, the sensitivity is far superior to previous methods.

### 3.4 Analysis of oligosaccharides in glycoproteins

The resolution of AMC-labeled oligosaccharides was evaluated using a series of  $\alpha_1,6$ -linked glucose oligomers called isomaltooligosaccharides, which had DPs distributed from 1 to 20 or more. Boric acid forms a stable complex with the linear polyalcohol structure at linear monosaccharide residues linked to AMC and the binding ability of borate to ring-formed monosaccharide residues is not high. They migrated in the

order of increasing DP because of the low mobility of oligosaccharides due to the low binding capability to borate ions. To enhance the apparent mobility of AMC-oligosaccharides, we chose 250 mM potassium borate buffer (pH 9.0). As shown in Fig. 5A, they were completely resolved and oligosaccharides corresponding to DPs of more than 20 were detected within 60 min. Most N-linked oligosaccharides in glycoproteins are distributed between DPs of 7 and 20, which indicate that it is possible to separate a neutral oligosaccharide mixture of glycoproteins by this mode.

The separation conditions were applied to the analysis of AMC-labeled N-linked oligosaccharides from transferrin, fetuin, and ribonuclease B. However, the separation of acidic oligosaccharides derived from transferrin and fetuin indicates finer resolution using a somewhat lower pH of borate



**Figure 5.** Separation of a mixture of isomaltooligosaccharides (A), ribonuclease B (B), transferrin (C), and fetuin (D). BGE, 1:9, v/v, mixture of ACN and borate buffer containing 0.5% hydroxypropylcellulose; 250 mM potassium borate (pH 9.0) for (A) and (B), and 100 mM Tris borate (pH 8.5) for (C) and (D), respectively.

buffer. Therefore, we applied 100 mM Tris borate (pH 8.5) for acidic oligosaccharide separation and 250 mM potassium borate buffer (pH 9.0) for neutral oligosaccharides. Results are shown in Fig. 5B–D. Oligosaccharide structures in each peak indicate there was identification based on co-migration of an AMC-oligosaccharide pool prepared by HPLC fractionation [14].

RNB contains a series of high-mannose type oligosaccharides. Their separation profile (Fig. 5B) indicates they migrated in order of their size,  $\text{Man}_5$  to  $\text{Man}_9$ . However the separation mode could not separate linkage isomers of  $\text{Man}_7$  and  $\text{Man}_8$  high-mannose type oligosaccharides.

Oligosaccharides of transferrin (Fig. 5C) are mainly composed from disialylated biantennary oligosaccharides, which appeared as a large peak at 20.5 min. The subsequent small

peaks should be assigned to fucosylated biantennary oligosaccharides.

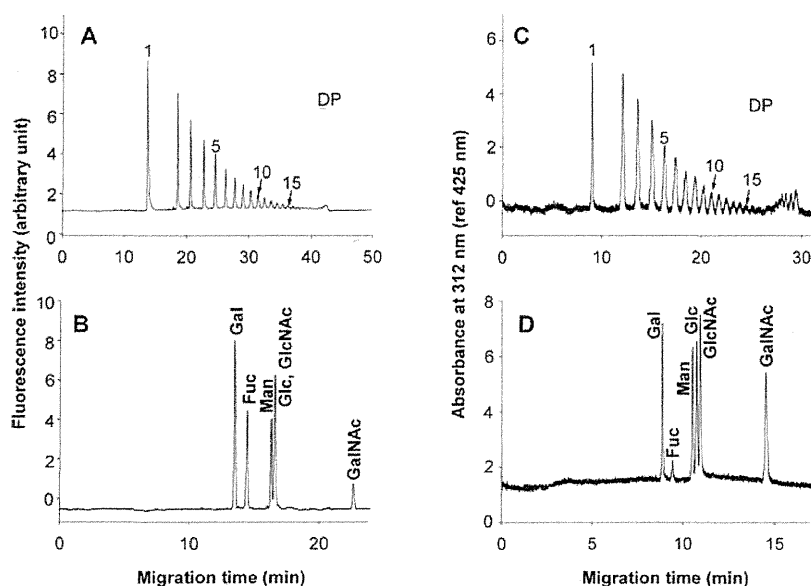
Fetuin mainly contains a series of di-, tri-, and tetra-sialylated triantennary glycans with variation in the linkage isomers of neuraminic acids and the presence of the Lewis X-type branch in the  $\alpha 1,4$ -linked Gal–GlcNAc branch. As shown in Fig. 5D, AMC oligosaccharides from fetuin were mainly separated according to the number of sialic acids and were further resolved by the linkage type and position as well as differences in the lactosamine linkage. The peaks detected at 14, 17, and 20–22 min correspond to tetra-, tri-, and disialylated oligosaccharides. Furthermore, four peaks appearing at 20–22 min correspond to biantennary and triantennary di-sialylated oligosaccharides. Di-sialylated triantennary oligosaccharides may be generated from partial loss of a sialic acid from triantennary oligosaccharides, which causes numerous linkage isomers and appeared as a broad peak at 22 min. Unfortunately, this separation mode is not suitable for the resolution of these oligosaccharide isomers.

### 3.5 Application to the separation of saccharides using other labels

Finally, as a practical test, monosaccharide mixtures and isomaltooligosaccharides were labeled with AMAC and ABEE, and the derivatives were subjected to separation with borate complex mode CE, as shown in Figs. 5A and 1B, respectively. As shown in Fig. 6, AMAC- and ABEE-labeled saccharides showed an essentially identical pattern to AMC saccharides and were also free from interference by excess reagents. ABEE derivatives migrated faster than those of AMAC derivatives so the resolution of AMAC-oligosaccharides was high. The resolution of the Glc and GlcNAc pair was achieved using ABEE derivatives. We also evaluated these separation conditions for other labels, such as *p*-aminobenzonitrile (ABN) and 5-amino-1-naphthol (AN). However, the reaction products of isomaltooligosaccharides and ABN showed an intense, unknown signal at ca. 5 min, and that of AN showed an unknown peak at 15 min (data not shown). We speculate that these peaks may be due to the products of degradation of reagents, generated during derivatization reactions.

## 4 Concluding remarks

A combination of alkaline borate buffer and a neutrally coated capillary enables specific determination of AMC-labeled oligosaccharides, and an LED-based fluorimetric detection was applied to sub-amol level detection of saccharides. This method enables analysis without removal of excess reagents from the reaction mixture, enabling reliable quantitative analysis of monosaccharides in hydrolysates of several glycoproteins. This separation mode is also applicable to oligosaccharides that are released from glycoproteins. The separation conditions are also applicable to other labeled saccharides. Therefore, our methods are applicable to most



**Figure 6.** Application to the separation of isomaltooligosaccharides and monosaccharide mixtures labeled with AMAC (A, B) and ABEE (C, D). Analytical conditions for (A) and (C) were the same as those for Fig. 3 (A, B), while those for (B) and (D) were the same as those for Fig. 1 (B). AMAC derivatives were detected at 488 (ex)/522 (em) nm. ABEE derivatives were monitored by absorption at 210 nm.

reductively aminated saccharides, using neutral or basic labeling dyes without interference by excess reagents.

This work was supported by a Grant-in-Aid for Scientific Research (C) from the Japan Society for the Promotion of Science (JSPS), Japan, 2007–2011.

The authors have declared no conflict of interest.

## 5 References

- [1] Anumula, K. R., *Anal. Biochem.* 2006, **350**, 1–23.
- [2] Harvey, D. J., *J. Chromatogr.* 2011, **B 879**, 1196–1225.
- [3] Vanderschaeghe, D., Festjens, N., Delanghe, J., Callewaert, N., *Biol. Chem.* 2010, **391**, 149–161.
- [4] Briggs, J. B., Keck, R. G., Ma, S., Lau, W., Jones, A. J., *Anal. Biochem.* 2009, **389**, 40–51.
- [5] Chen, F. T., Evangelista, R. A., *Electrophoresis* 1998, **19**, 2639–2644.
- [6] Guttman, A., *Electrophoresis* 1997, **18**, 1136–1141.
- [7] Huang, Y., Mechref, Y., Novotny, M. V., *Anal. Chem.* 2001, **73**, 6063–6069.
- [8] Yagi, Y., Yamamoto, S., Kakehi, K., Hayakawa, T., Ohyama, Y., Suzuki, S., *Electrophoresis* 2011, **32**, 2979–2985.
- [9] Hase, S., Ikenaka, T., Matsushima, Y., *J. Biochem.* 1981, **90**, 407–414.
- [10] Nakagawa, H., Kawamura, Y., Kato, K., Shimada, I., Arata, Y., Takahashi, N., *Anal. Biochem.* 1995, **226**, 130–138.
- [11] Takahashi, N., Khoo, K. H., Suzuki, N., Johnson, J. R., Lee, Y. C., *J. Biol. Chem.* 2001, **276**, 23230–23239.
- [12] Tomiya, N., Kurono, M., Ishihara, H., Tejima, S., Endo, S., Arata, Y., Takahashi, N., *Anal. Biochem.* 1987, **163**, 489–499.
- [13] Yodoshi, M., Oyama, T., Masaki, K., Kakehi, K., Hayakawa, T., Suzuki, S., *Anal. Sci.* 2011, **27**, 395–400.
- [14] Yodoshi, M., Tani, A., Ohta, Y., Suzuki, S., *J. Chromatogr. A* 2008, **1203**, 137–145.
- [15] Honda, S., Suzuki, S., *Anal. Biochem.* 1984, **142**, 167–174.
- [16] Birrell, H., Charlwood, J., Lynch, I., North, S., Camilleri, P., *Anal. Chem.* 1999, **71**, 102–108.
- [17] Wang, W. T., Ledonne, N. C., Ackerman, B., Sweeley, C. C., *Anal. Biochem.* 1984, **141**, 366–381.
- [18] Suzuki, S., Honda, S., *Electrophoresis* 1998, **19**, 2539–2560.
- [19] Hoffstetter-Kuhn, S., Paulus, A., Gassmann, E., Widmer, H. M., *Anal. Chem.* 1991, **63**, 1541–1547.
- [20] Honda, S., Suzuki, S., Kakehi, K., *J. Chromatogr.* 1981, **226**, 341–350.
- [21] Fournet, B., Montreuil, J., Strecker, G., Dorland, L., Haverkamp, J., Vliegthart, J. F. G., Binette, P., Schmid, K., *Biochemistry* 1978, **17**, 5206–5214.
- [22] Nakano, M., Kakehi, K., Tsai, M. H., Lee, Y. C., *Glycobiology* 2004, **14**, 431–441.
- [23] Townsend, R. R., Hardy, M. R., Cumming, D. A., Carver, J. P., Bendiak, B., *Anal. Biochem.* 1989, **182**, 1–8.
- [24] Spiro, R. G., Bhoyroo, V. D., *J. Biol. Chem.* 1974, **249**, 5704–5717.
- [25] Green, E. D., Adelt, G., Baenziger, J. U., Wilson, S., Van Halbeek, H., *J. Biol. Chem.* 1988, **263**, 18253–18268.
- [26] Tai, T., Yamashita, K., Ito, S., Kobata, A., *J. Biol. Chem.* 1977, **252**, 6687–6694.
- [27] Tai, T., Yamashita, K., Ogata-Arakawa, M., Koide, N., Muramatsu, T., Iwashita, S., Inoue, Y., Kobata, A., *J. Biol. Chem.* 1975, **280**, 8569–8575.
- [28] Yamashita, K., Tachibana, Y., Kobata, A., *J. Biol. Chem.* 1978, **253**, 3862–3869.
- [29] Koller, A., Khandurina, J., Li, J., Kreps, J., Schieltz, D., Guttman, A., *Electrophoresis* 2004, **25**, 2003–2009.
- [30] Honda, S., Akao, E., Suzuki, S., Okuda, M., Kakehi, K., Nakamura, J., *Anal. Biochem.* 1989, **180**, 351–357.

## Common Glycoproteins Expressing Polylactosamine-Type Glycans on Matched Patient Primary and Metastatic Melanoma Cells Show Different Glycan Profiles

Mitsuhiro Kinoshita,<sup>†</sup> Yosuke Mitsui,<sup>†</sup> Naotaka Kakoi,<sup>†</sup> Keita Yamada,<sup>†</sup> Takao Hayakawa,<sup>‡</sup> and Kazuaki Kakehi<sup>\*†</sup>

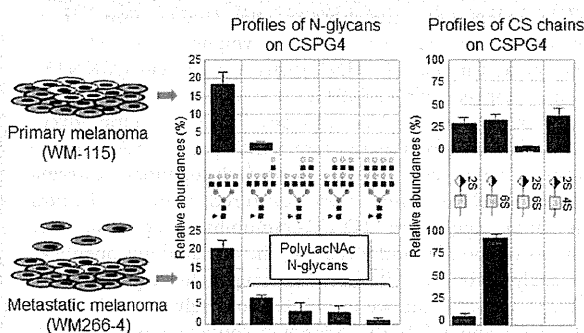
<sup>†</sup>School of Pharmacy, Kinki University, Kowakae 3-4-1, Higashi-Osaka 577-8502, Japan

<sup>‡</sup>Pharmaceutical Research and Technology Institute, Kinki University, Kowakae 3-4-1, Higashi-Osaka 577-8502, Japan

### Supporting Information

**ABSTRACT:** Recently, we reported comparative analysis of glycoproteins which express cancer-specific *N*-glycans on various cancer cells and identified 24 glycoproteins having polylactosamine (polyLacNAc)-type *N*-glycans that are abundantly present in malignant cells [Mitsui et al., *J. Pharm. Biomed. Anal.* 2012, 70, 718–726]. In the present study, we applied the technique to comparative studies on common glycoproteins present in the matched patient primary and metastatic melanoma cell lines. Metastatic melanoma cells (WM266-4) contained a large amount of polyLacNAc-type *N*-glycans in comparison with primary melanoma cells (WM115). To identify the glycoproteins expressing these *N*-glycans, glycopeptides having polyLacNAc-type *N*-glycans were captured by a *Datura stramonium* agglutinin (DSA)-immobilized agarose column. The captured glycopeptides were analyzed by LC/MS after removing *N*-glycans, and some glycoproteins such as basigin, lysosome-associated membrane protein-1 (LAMP-1), and chondroitin sulfate proteoglycan 4 (CSPG4) were identified in both WM115 and WM266-4 cells. The expression level of polyLacNAc of CSPG4 in WM266-4 cells was significantly higher than that in WM115 cells. In addition, sulfation patterns of chondroitin sulfate (CS) chains in CSPG4 showed dramatic changes between these cell lines. These data show that characteristic glycans attached to common proteins observed in different stages of cancer cells will be useful markers for determining degree of malignancies of tumor cells.

**KEYWORDS:** polylactosamine, chondroitin sulfate, melanoma, malignant transformation



### INTRODUCTION

Glycosylation is one of the frequently observed post-translational modifications of proteins and plays various important roles such as protein folding, cellular communications, and signal transductions.<sup>1,2</sup> It is also well-known that embryonic development and cellular activation in mammalian cells are often accompanied by alterations in glycosylation. In addition, aberrant glycosylation has been known to be associated with various human diseases.<sup>3–7</sup> Expression of GlcNAc transferase V (GlcNAcT-V), which is the rate-limiting enzyme for the synthesis of polylactosamine (tandem repeating units of Gal $\beta$ 1-4GlcNAc at the nonreducing terminal ends), is increased in numerous cancer cells to cause increases of polyLacNAc-carrying *N*-glycans.<sup>8–11</sup> Colon cancer cells highly express sialyl-Lewis<sup>x</sup> (NeuAc $\alpha$ 2-3Gal $\beta$ 1-4[Fuc $\alpha$ 1-3] GlcNAc-R), while they show markedly decreased level of sialyl 6-sulfo Lewis<sup>x</sup> compared with normal colonic cells.<sup>12</sup> Thus, alterations in glycosylation are a universal hallmark and prominent biomarkers for cancer.

Serological assays detect carbohydrate antigens such as sialyl-Lewis<sup>x</sup>, sialyl-Le<sup>a</sup> (CA19-9) and MUC16 (CA125). Sialyl-Lewis<sup>x</sup> is a weak marker for some small-cell lung cancers (24% for all stages), however, sialyl-Lewis<sup>x</sup> increases with tumor progression (71% for late-stage).<sup>13</sup> Unfortunately, elevation of these carbohydrate antigens is only suggestive of a cancer.  $\alpha$ -Fetoprotein (AFP) is a well-known biomarker for liver diseases (e.g., cirrhosis, hepatitis, and hepatocellular carcinoma (HCC)), but its specificity for diagnosis of HCC is low (less than 50%). In contrast, fucosylated AFP (AFP-L3) is particularly useful in early detection of aggressive tumors associated with HCC with high specificity (>95%).<sup>14</sup> Alteration of serum  $\alpha$ 1-acid glycoprotein (AGP) has been reported to be associated with a risk of developing HCC during cirrhosis in chronic hepatitis. Kuno et al. statistically evaluated the relationship between the progression of liver fibrosis during cirrhosis and the decreased

Received: October 8, 2013

Published: December 19, 2013

$\alpha$ 2–3 sialylation/the increased core  $\alpha$ 1-6fucosylation of *N*-glycans in AGP.<sup>15</sup>

Although time-consuming and laborious analysis is required for finding a candidate for cancer-specific biomarkers, detailed analysis of glycans in glycoconjugates provides us useful information for the development of novel biomarkers. In our previous reports, we proposed a series of methods for the analysis of glycans of glycoproteins in cancer cells.<sup>16,17</sup> Total glycan pool obtained from the cells was fluorescently labeled with 2-aminobenzoic acid (2-AA) and separated based on the number of sialic acid residues attached to the glycans using affinity chromatography on a serotonin-immobilized stationary phase. Total amounts of glycans as well as those of each category of glycans (asialo/high-mannose, mono-, di-, tri-, and tetra-sialoglycans) were determined based on their fluorescent intensities. This is very important information for determination of the expressed level of each category of the glycans. Then, the collected glycan groups were extensively analyzed by MS<sup>n</sup> technique. On the basis of the studies using these techniques, we found that histiocytic lymphoma cells (U937), kidney glandular cells (ACHN), gastric cancer cells (MKN45), and lung cancer cells (A549) express a large amount of *N*-glycans having polyLacNAc residues.<sup>16,17</sup> To confirm glycoproteins which express these characteristic polyLacNAc-type *N*-glycans in cancer cells, tryptic-digested glycopeptides carrying multiple LacNAc units were captured using a *Datura stramonium* agglutinin (DSA)-immobilized column. The positions of peptides and glycans of the captured glycopeptides were analyzed by LC/MS<sup>n</sup>-based technique after digestion with *N*-glycoamidase F, and we found that some glycoproteins such as CD107a and CD107b commonly contained polyLacNAc-type *N*-glycans in all the examined cancer cells. But integrin- $\alpha$ 5 (CD49e) and carcinoembryonic antigen-related cell adhesion molecule 5 (CD66e) having these glycans were specifically found in U937 and MKN45 cells, respectively. These data indicate that specific glycans attached to specific proteins will be promising markers for specific tumors with high accuracy.<sup>18</sup>

Melanoma consists of an invasive tumors that are resistant to conventional therapy.<sup>19</sup> Therefore, monitoring of high-risk patients at early stage is highly recommended, but biomarkers for melanoma identification, prediction of progression, and prognosis are lacking. Although measurement of serum lactate dehydrogenase (LDH) is used for staging of melanoma, it is not specific for melanoma and cannot be used to predict progression or prognosis.<sup>19</sup> Melanoma inhibitory activity (MIA), a 11 kDa soluble protein, is present in the supernatant of the human melanoma cell line (HTZ-19). However, increased MIA levels are also observed in a subset of the patients with ovarian, pancreatic, breast, and colon cancer.<sup>20</sup> 5-S-Cysteinyldopa (5-S-CD) is produced in melanocytes and melanoma cells and has been reported to be raised particularly in late-stage (stage III and IV).<sup>20</sup> Thus, these biomarkers are detected frequently in the advanced stages of melanomas but are not useful for monitoring of stages or early detection of melanoma progression.

In the present study, we performed comparative studies on common glycoproteins present in the matched patient primary and metastatic melanoma cell lines, WM115 and WM266-4. At the initial step, total *N*-glycans expressed in both melanoma cells were comprehensively analyzed. Subsequently, glycoproteins having characteristic *N*-glycans that were observed in both cell lines were identified by combination of lectin-affinity capturing and bottom-up proteomics approaches. Among

identified glycoproteins, chondroitin sulfate proteoglycan 4 (CSPG4) having both *N*-glycans and glycosaminoglycans (GAGs) was confirmed as a convincing marker for the melanoma-specific glycoproteins, and the structures of *N*-glycans and glycosaminoglycans of CSPG4 from each cell line were studied in detail.

## MATERIALS AND METHODS

### Materials

Peptide *N*-glycoamidase F (EC 3.5.1.52) was obtained from Roche Diagnostics (Mannheim, Germany). Neuraminidase (*Arthrobacter ureafaciens*) was kindly donated by Dr. Ohta (Marukin-Bio, Uji, Kyoto, Japan). Benzonase was obtained from Novagen (Darmstadt, Germany). TPCK-treated trypsin was from Worthington (Lakewood, NJ). Anti-LAMP-1 (H4B3) mouse IgG1 monoclonal, and anti-CSPG4 (LHM2) mouse IgG monoclonal were from Santa Cruz Biotechnology (Santa Cruz, CA). Anti-Basigin (MEM-M6/1) mouse IgG1 monoclonal was from Abcam (Cambridge, U.K.). Iodoacetamide was from Tokyo Kasei Kogyo (Chuo-ku, Tokyo, Japan). Dithiothreitol (DTT) was obtained from Nacalai Tesque (Nakagyo-ku, Kyoto, Japan). 3,3'-Diaminobenzidine tetrahydrochloride (DAB) was obtained from DOJINDO (Kamimashiki-gun, Kumamoto, Japan). 2-Aminobenzoic acid (2-AA) and sodium cyanoborohydride for fluorescent labeling of oligosaccharides were from Tokyo Kasei. Coomassie brilliant blue G-250 was purchased from BIO-RAD (Hercules, CA). Sephadex LH-20 was from Amersham Bioscience (Uppsala, Sweden). Vivaspin 500 was obtained from Sartorius (Goettingen, Germany). *Datura stramonium* agglutinin (DSA)-agarose, chondroitinase ABC, and standard samples of unsaturated disaccharides derived from glycosaminoglycans were obtained from Seikagaku Kogyo (Chuoku, Tokyo, Japan). VECTA Elite ABC mouse IgG kit for Western blotting was obtained from Vector Laboratories (Burlingame, CA). Immobilon-P transfer membrane (PVDF) was from Millipore (Bedford, MA). Protein inhibitor cocktail for animal cells was obtained from Nacalai Tesque. Protein G Sepharose 4 Fast Flow was obtained from GE Healthcare (Uppsala, Sweden). All other reagents and solvents were of the highest grade commercially available or of HPLC grade. All aqueous solutions were prepared using water purified with a Milli-Q purification system (Millipore, Bedford, MA).

### Cell Culture

WM266-4 (human metastatic melanoma cells) and WM115 cells (human primary melanoma cells) derived from a same patient were employed as the materials. Both cells were cultured at 37 °C under 5% CO<sub>2</sub> atm in EMEM medium supplemented with 10% (v/v) fetal bovine serum, 2 mM glutamine, 1% nonessential amino acids (NEAA), and 1% sodium pyruvate. The cells were harvested at 80% confluent state, washed with phosphate buffered saline (PBS), and collected by centrifugation at 1000 rpm for 20 min.

### Whole Proteins from Melanoma Cell Lines

Melanoma cells (1.0 × 10<sup>7</sup> cells) were suspended in PBS (50  $\mu$ L) containing 1 mM EDTA and kept at room temperature for 15 min. Extraction reagent (7 M urea, 2 M thiourea, 4% CHAPS, 30 mM Tris-HCl (pH 8.5, 268  $\mu$ L)), 1 M DTT (17  $\mu$ L), and benzonase (125 units, 5  $\mu$ L) were added to the suspended cells and kept at 37 °C for 30 min. The mixture was centrifuged at 8000g for 15 min. After addition of acetone

solution (85% acetone, 5% triethylamine, 5% acetic acid in water (1.7 mL)), the mixture was kept at  $-20^{\circ}\text{C}$  for 30 min and the precipitate was collected by centrifugation at 8000g for 15 min and washed with 75% ethanol (1 mL  $\times$  2). The precipitate was dried by a centrifugal evaporator.

#### Release of *N*-Glycans from Glycoproteins and Fluorescent Labeling of the Released *N*-Glycans with 2-Aminobenzoic acid (2-AA)

The whole protein pool obtained as described above was suspended in water (210  $\mu\text{L}$ ), 10% SDS (24  $\mu\text{L}$ ), and 2-mercaptoethanol (2.4  $\mu\text{L}$ ). The mixture was kept in the boiling water bath for 10 min. After cooling, 10% NP-40 solution (24  $\mu\text{L}$ ) and 1 M phosphate buffer (pH 7.5, 29  $\mu\text{L}$ ) were added. *N*-Glycoamidase F (4 U/4  $\mu\text{L}$ ) was added to the mixture and incubated at  $37^{\circ}\text{C}$  for 24 h. After keeping the mixture in the boiling water bath for 5 min, the mixture was mixed with 695  $\mu\text{L}$  of EtOH and centrifuged at 12000g for 15 min. The supernatant containing the released *N*-glycans was collected followed by lyophilization to dryness by a centrifugal evaporator. The dried mixture was dissolved in 2-AA (200  $\mu\text{L}$ ) solution prepared by dissolution of 2-AA (30 mg) and sodium cyanoborohydride (30 mg) in methanol (1 mL) containing 4% sodium acetate and 2% boric acid. The mixture was kept at  $80^{\circ}\text{C}$  for 60 min. After addition of distilled water (200  $\mu\text{L}$ ), the mixture was applied to a column of Sephadex LH-20 (1.0 cm i.d., 30 cm length) equilibrated with 50% aqueous MeOH. The earlier eluted fluorescent fractions were collected and evaporated to dryness. The dried residue was dissolved in distilled water and used for the analysis of *N*-glycans.

#### Group Separation of 2-AA-Labeled *N*-Glycans Based on the Number of Sialic Acid Residues by Serotonin-Affinity Chromatography

Serotonin-affinity chromatography was performed by a Jasco HPLC apparatus equipped with two PU980 pumps and a Jasco FP920 fluorescence detector (Hachio-ji, Tokyo, Japan). An aqueous solution of the mixture of 2-AA-labeled *N*-glycans (10  $\mu\text{L}$ , corresponded to  $2.0 \times 10^6$  cells) was separated based on the number of sialic acid residues using a serotonin-immobilized column (4.6 mm i.d.  $\times$  150 mm length, J-Oilmils, Chu-o ku, Tokyo, Japan) by linear gradient from water (eluent A) to 40 mM ammonium acetate (eluent B) at a flow rate of 0.5 mL/min. Initially, eluent B was used at 5% concentration for 2 min, and then linear gradient elution was performed to 75% eluent B for 35 min, and finally the eluent was changed to 100% eluent B during the following 10 min. Peaks were collected and lyophilized to dryness.

#### NP-HPLC Analysis of 2-AA-Labeled *N*-glycans

Each group of *N*-glycans obtained by serotonin-affinity chromatography was further separated by normal-phase high-performance liquid chromatography after removing sialic acids by digestion with neuraminidase. A portion (10  $\mu\text{L}$ , corresponded to  $5 \times 10^5$  cells) of asialoglycans was analyzed with an Amide-80 column (Tosoh, 4.6 mm  $\times$  250 mm) using a linear gradient formed by 0.2% acetic acid in acetonitrile (solvent A) and 0.5% acetic acid in water containing 0.3% triethylamine (solvent B). The column was initially equilibrated and eluted with 30% solvent B for 2 min, from which point solvent B was increased to 95% over 80 min and kept at this composition for further 100 min. Flow rate was kept at 1.0 mL/min. The observed peaks were collected and lyophilized to dryness for the analysis by matrix-assisted laser-desorption

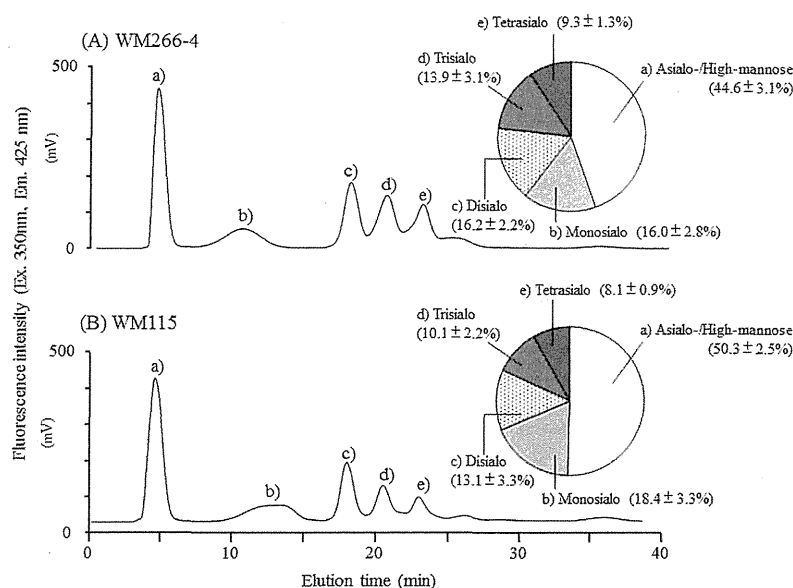
ionization time-of-flight (MALDI-TOF) mass spectrometry (MS) according to the previous papers.<sup>17,18</sup> All *m/z* values of *N*-glycans were investigated using "Glyco-Peakfinder", which is a tool for annotation of glycan on MS-spectra (EuroCarbDB).

#### Lectin Affinity Chromatography of Glycopeptides Using a DSA-Immobilized Agarose Column

The whole protein pool from melanoma cells ( $1.0 \times 10^7$  cells) was dissolved in guanidine solution (2 mM EDTA, 0.5 M Tris-HCl, and 4 M guanidine (pH 8.5, 80  $\mu\text{L}$ )), and 0.18 M DTT in guanidine solution (40  $\mu\text{L}$ ) was added to the mixture. The mixture was kept at  $37^{\circ}\text{C}$  for 90 min. After addition of 0.18 M iodoacetamide in guanidine solution (55  $\mu\text{L}$ ), the mixture was kept for 45 min in a dark place. After addition of acetone solution (85% acetone, 5% triethylamine, 5% acetic acid in water (1.7 mL)), the mixture was kept at  $-20^{\circ}\text{C}$  for 30 min. The precipitate was collected by centrifugation at 8000g for 15 min and washed with 75% ethanol (1 mL  $\times$  2) and dried by a centrifugal evaporator. The dried material was digested with TPCK-treated trypsin (100  $\mu\text{g}$ ) in 0.1 M Tris-HCl (pH 8.6, 800  $\mu\text{L}$ ) containing 2 M urea at  $37^{\circ}\text{C}$  overnight. After keeping the mixture at  $100^{\circ}\text{C}$  for 10 min, the supernatant was collected and passed through an ultrafiltration membrane (MW cut off, 5000 Da). The residual solution on the membrane was used as a mixture of glycopeptides and applied to a DSA-immobilized column (DSA 3.8 mg (7.9 nmol)/1 mL of agarose), which had been previously equilibrated with PBS. Unbound peptides were eluted with PBS (15 mL). Then the bound glycopeptides were eluted with 0.1 M *N*-acetyl D-glucosamine in PBS (15 mL). The bound and unbound fractions were passed through an ultrafiltration membrane (MWCO, 3000 Da), respectively. The residual solutions on the membrane were evaporated to dryness by a centrifugal evaporator. DSA-bound/unbound glycopeptides were suspended in a mixture of water (210  $\mu\text{L}$ ), 10% SDS (24  $\mu\text{L}$ ), and 2-mercaptoethanol (2.4  $\mu\text{L}$ ) and was kept in the boiling water bath for 10 min. After cooling, 10% NP-40 solution (24  $\mu\text{L}$ ) and 1 M phosphate buffer (pH 7.5, 29  $\mu\text{L}$ ) were added. *N*-Glycoamidase F (4 U/4  $\mu\text{L}$ ) was added to the mixtures and kept at  $37^{\circ}\text{C}$  for 24 h. After keeping the mixtures in the boiling water bath for 5 min followed by centrifugation at 8000g for 10 min, the supernatant solutions were collected. One half of the solutions were used for the analysis of de-*N*-glycosylated peptides, and another half were used for the analysis of *N*-glycans after fluorescent labeling with 2-AA in the same manner as describe above.

#### Liquid Chromatography (LC)-Ion-Trap Time-of-Flight (IT-TOF) MS Analysis of Peptides

Positive electrospray ionization (ESI)-MS analyses were conducted with an LC-IT-TOF MS instrument (Shimadzu, Kyoto) connected with an HPLC system (two LC-20AD pumps, a CTO-20AC column oven, and a CBM-20A system controller; Shimadzu, Kyoto). A portion (3  $\mu\text{L}$ , equivalent to  $5 \times 10^6$  cells) of the aqueous solution of the peptide mixture obtained by digestion with *N*-glycoamidase F was injected to a reverse-phase column (HiQ sil C18 column, 2.1 mm  $\times$  150 mm; KYA TECH) and analyzed using the following gradient program. Solvent A was 5% acetonitrile/0.1% formic acid. Solvent B was 95% acetonitrile/0.1% formic acid. The column was initially equilibrated and eluted with 5% solvent B for 5 min, from which point solvent B was increased to 75% over 30 min at a flow rate of 0.2 mL/min. Column temperature was kept at  $40^{\circ}\text{C}$ . The MS apparatus was operated at a probe voltage of 4.50 kV, CDL temperature of  $200^{\circ}\text{C}$ , nebulizer gas



**Figure 1.** Serotonin-affinity chromatography of *N*-glycans derived from WM266-4 (A) and WM115 (B) cells. Analytical conditions: column, a serotonin-immobilized column (4.6 mm i.d., 150 mm length); eluent A, distilled water; eluent B, 40 mM ammonium acetate; gradient condition, linear gradient from 5% of eluent B to 75% of eluent B (2–37 min), and 75% of eluent B to 100% of eluent B for 10 min; flow rate, 0.5 mL/min; column temperature, 30 °C. Peak (a) asialo-/high mannose-type glycans, peak (b) monosialo-glycans, peak (c) disialo-glycans, peak (d) trisialo-glycans, peak (e) tetrasialo-glycan. The data in pie graphs were obtained by three experimental data.

flow of 1.5 L/min, and ion accumulation time of 30 ms. MS range was from *m/z* 200 to 2000, and MS/MS range also from *m/z* 200 to 2000. CID parameters were as follows: energy, 50%; collision gas, 50%. Monoisotopic ion was used as the precursor ion. MS data were processed with LCMS solution software ver. 3.6 (Shimadzu).

#### Peptide Mass Finger Printing

MS/MS spectra were processed using LCMS solution software version 3.6 (Shimadzu), and peak list files (Mascot generic format) for MS/MS ion search were generated using Mascot Distiller (version 2.3, Matrix Science). The parameters for database search were as follows. Protein database was set to Swiss PROT (version, 2011\_12 containing 20323 human protein sequences). Taxonomy was set to *Homo sapiens*. One trypsin missed cleavage was allowed. The mass tolerance was set to 0.5 Da for precursor ions and 0.5 Da for product ions. Carbamidomethyl (C) was chosen as a fixed modification. Deamidated (NQ) was chosen for de-*N*-glycosylation (Asn (N) to Asp (D)). Peptide charge was chosen as +1, +2, and +3. Data format was chosen as Mascot generic, and instrument was chosen as ESI-TRAP-TOF. A decoy search (based on automatically generated random sequences) was employed to determine the false discovery rate (FDR) in MS/MS-based identification. The FDR was an average of 2.12% for all experiments.

#### Sodium Dodecyl Sulfate-Polyacrylamide Gel Electrophoresis (SDS-PAGE)

After addition of SDS-PAGE sample buffer (250 mM Tris-HCl (pH 6.8)-4.6% SDS, 20% glycerol), 2-mercaptoethanol, and water (10:9:1, 2  $\mu$ L) to the whole protein ( $1 \times 10^7$  cells), the mixture was vortexed and boiled for 10 min. The supernatant was collected after centrifugation and used for SDS-PAGE. SDS-PAGE was performed with a Mini protean 3 cell and a POWER PAC 3000 (Bio Rad, Hercules, CA). The applied

protein was 25  $\mu$ g/lane as examined by the BCA method using bovine serum albumin as standard. Separation gel was 10%. Electrophoresis buffer was 25 mM Tris, 198 mM glycine, and 1% (w/v) SDS in water. After SDS-PAGE, the gel was stained with Coomassie brilliant blue G-250 (CBB) for 1 h. CBB solution contains 40% methanol, 10% acetic acid, and 0.2% CBB. The gel was destained with 40% methanol–10% acetic acid.

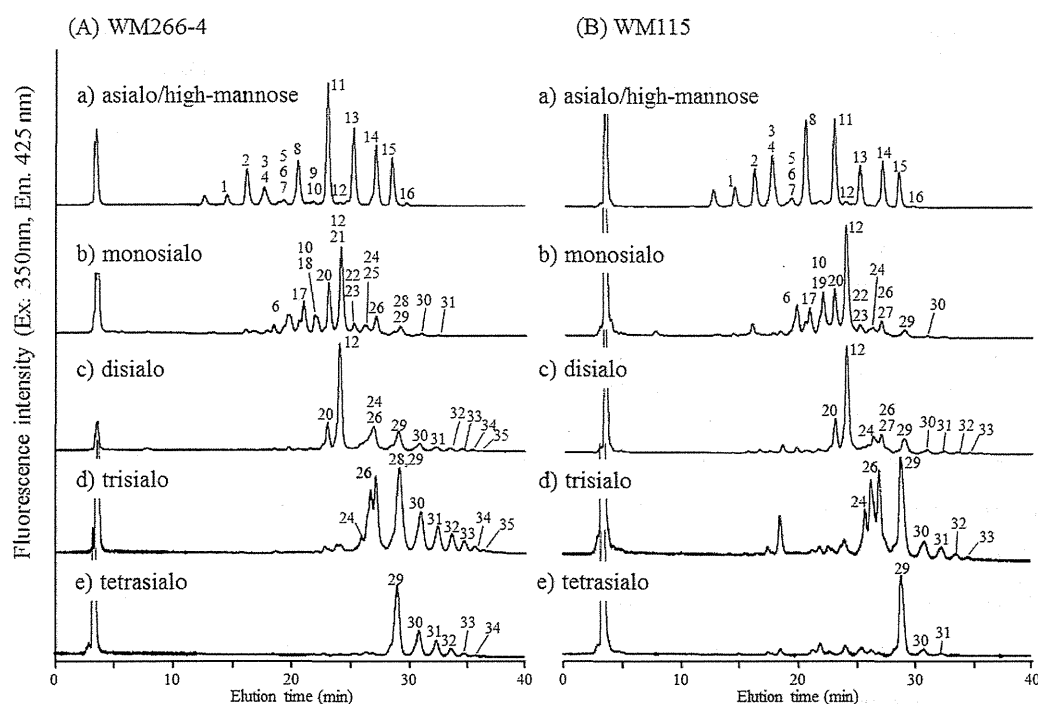
#### Western Blot Analysis

Western blot analysis was performed with a semidry electrophoretic transfer cell (Trans-Blot SD, BIO-RAD, Hercules, CA). PVDF membrane was previously kept in methanol for 1 min and in the blotting buffer (48 mM Tris, 39 mM glycine, and 20% methanol (pH9.0)) for 1 h. Each sample solution obtained as described above (25  $\mu$ g as protein) from WM266-4 and WM115 cells was resolved using reducing 10% SDS-PAGE, and transferred to a PVDF membrane. The membrane was incubated in blocking buffer (5% skim milk, 0.05% Tween 20 in PBS). After washing the membrane with 0.05% Tween 20/PBS (20 mL  $\times$  4), the membrane was reacted with a primary antibody overnight. All the primary antibodies were used at the same concentration (5  $\mu$ g/mL, 5 mL). After washing the membrane with 0.05% Tween 20/PBS (20 mL  $\times$  4), the membrane was reacted with the biotin conjugated secondary antibodies (5  $\mu$ g/mL, 5 mL) for 1 h. After washing with 0.05% Tween 20/PBS (20 mL), the PVDF membrane was reacted with HRP labeled avidin (5  $\mu$ g/mL, 5 mL in PBS) for 1 h. After washing with 0.05% Tween 20/PBS (20 mL  $\times$  4), the membrane was visualized with 0.05% DAB, 0.0031% hydrogen peroxide in 100 mM Tris-HCl buffer (pH 7.5).

#### Immunoprecipitation of Chondroitin Sulfate Proteoglycans 4 (CSPG4)

Anti-CSPG4 (50  $\mu$ g/mL, 100  $\mu$ L) was added to Protein G Sepharose (100  $\mu$ L), and the mixture was incubated for 1 h.





**Figure 2.** NP-HPLC analysis of five *N*-glycan fractions separated by serotonin-affinity chromatography. The *N*-glycans were previously digested with neuraminidase. Analytical conditions: column, TSK-Gel Amide-80 (4.6 mm  $\times$  250 mm); eluent A, 0.2% acetic acid/acetonitrile; eluent B, 0.5% acetic acid–0.3% triethylamine/water. Gradient elution, 0–2 min (30% solvent B), 2–82 min (30–95% solvent B), 82–102 min (95% solvent B). Detection, ex 350 nm, em 425 nm. Column temperature, 40 °C. The numbers on the peaks are those in the list of *N*-glycans of Table 1

Protein G Sepharose thus prepared was washed with PBS (1 mL  $\times$  3), and the protein mixture obtained from the cells (1  $\times$  10<sup>7</sup> cells, see above) was added. The mixture was incubated at 4 °C overnight with gentle swirling. Protein G Sepharose was washed with PBS (1 mL  $\times$  6). After addition of SDS sample buffer (20  $\mu$ L) and 2-mercaptoethanol (2  $\mu$ L), Protein G Sepharose was boiled for 10 min. One half of the supernatant was collected by centrifugation and used for SDS-PAGE analysis, and the other half was used for the analysis of unsaturated disaccharides using capillary electrophoresis.

#### In-Gel Digestion with *N*-Glycoamidase F

Protein fractions collected by immunoprecipitation were analyzed by SDS-PAGE followed by staining with CBB. After changing the destaining solution with water, the positions detected by Western blot were cut, and the gel pieces were kept in 30% acetonitrile (300  $\mu$ L  $\times$  2) for 30 min and dehydrated with acetonitrile (200  $\mu$ L  $\times$  2) for 10 min.<sup>18</sup> After drying, the gel pieces were digested with *N*-glycoamidase F (2 U/2  $\mu$ L) in 100 mM phosphate buffer (pH 7.5, 100  $\mu$ L) at 37 °C overnight as described previously.<sup>21</sup> *N*-Glycans thus released were extracted with water (200  $\mu$ L  $\times$  3) for 30 min, and the supernatant solution was used for labeling with 2-AA after evaporation to dryness.

#### Analysis of Unsaturated Disaccharides in CSPG4 Species Prepared by Immunoprecipitation from WM266-4 and WM115 Cells

A half of the fraction containing CSPG4 obtained by immunoprecipitation (see above) was dissolved in 50 mM Tris-HCl buffer (pH 8.0, 100  $\mu$ L). Chondroitinase ABC (0.5 U) dissolved in the same buffer (10  $\mu$ L) was added to the

solution, and the mixture was kept at 37 °C for 12 h. The mixture of the unsaturated disaccharides thus eliminated was labeled with 2-AA according to the previously reported method<sup>22</sup> and analyzed by CE with a P/ACE MDQ Glycoprotein system (Beckman Coulter, Fullerton, CA, USA) equipped with a helium–cadmium laser-induced fluorescence detector (excitation 325 nm, emission 405 nm) using a fused silica capillary (50  $\mu$ m i.d., 30 cm) in 0.1 M Tris-phosphate buffer (pH 3.0). Sample solutions were introduced into the capillary by pressure injection at 1 psi for 5 s and analyzed by applying voltage of –25 kV at 25 °C. Peaks observed on the electropherograms were assigned by coinjection with a mixture of standard unsaturated disaccharides ( $\Delta$ diCS-0S,  $\Delta$ diHA-0S,  $\Delta$ diCS-4S,  $\Delta$ diCS-6S,  $\Delta$ diCS-di2,6S,  $\Delta$ diCS-di2,4S,  $\Delta$ diCS-di4,6S, and  $\Delta$ diCS-tri2,4,6S).

## RESULTS AND DISCUSSION

### Comparative Analysis of *N*-Glycans Expressed on WM266-4 and WM115 Cells

Total *N*-glycans prepared from WM266-4 and WM115 cells were separated based on the number of sialic acid residues using a serotonin-immobilized column as reported previously.<sup>16,17</sup> As shown in Figure 1, asialo-/high mannose-type *N*-glycans (peaks a) were not retained on the column and observed at ca. 5 min.

Monosialo- (peak b), disialo- (peak c), trisialo- (peak d), and tetrasialo- (peak e) *N*-glycans were observed at ca. 10–15 min, 18 min, 20 min, and 23 min, respectively. Asialo and high-mannose fractions were most abundant in both WM266-4 (44.6  $\pm$  3.1%) and WM115 (50.3  $\pm$  2.5%) cells. Relative abundances (18.4  $\pm$  3.3%) of monosialo *N*-glycans in WM115

Table 1. List of *N*-Glycans Expressed on WM266-4 and WM115 Cells

no.	structure <sup>a</sup>	observed m/z WM266-4/115	monosaccharide composition	relative abundances (%) to total <i>N</i> -glycans <sup>b</sup>											
				WM266-4 cells					sum of (a-e)	WM115 cells					sum of (a-e)
				(a)	(b)	(c)	(d)	(e)		(a)	(b)	(c)	(d)	(e)	
1		1030.41/1030.34	Man <sub>3</sub> GlcNAc <sub>2</sub> -2AA	1.38	-	-	-	-	1.38	2.91	-	-	-	-	2.91
2		1176.42/1176.29	Fuc <sub>1</sub> Man <sub>3</sub> GlcNAc <sub>2</sub> -2AA	5.12	-	-	-	-	5.12	5.70	-	-	-	-	5.70
3		1379.44/1379.52	Fuc <sub>1</sub> Man <sub>3</sub> GlcNAc <sub>3</sub> -2AA	1.18	-	-	-	-	1.18	3.84	-	-	-	-	3.84
4		1192.42/1192.49	Man <sub>4</sub> GlcNAc <sub>2</sub> -2AA	1.19	-	-	-	-	1.19	3.81	-	-	-	-	0.42
5		1338.39/1338.52	Fuc <sub>1</sub> Man <sub>4</sub> GlcNAc <sub>2</sub> -2AA	0.59	-	-	-	-	0.59	0.42	-	-	-	-	0.42
6		1395.38/1395.37	Gal <sub>1</sub> Man <sub>3</sub> GlcNAc <sub>3</sub> -2AA	0.44	0.99	-	-	-	1.43	0.53	1.78	-	-	-	2.31
7		1436.44/1436.51	Man <sub>3</sub> GlcNAc <sub>4</sub> -2AA	0.43	-	-	-	-	0.43	0.50	-	-	-	-	0.50
8		1354.35/1354.34	Man <sub>3</sub> GlcNAc <sub>2</sub> -2AA	6.50	-	-	-	-	6.50	13.68	-	-	-	-	13.68
9		1639.49/1639.38	Man <sub>3</sub> GlcNAc <sub>5</sub> -2AA	0.39	-	-	-	-	0.39	-	-	-	-	-	-
10		1744.49/1744.62	Gal <sub>1</sub> Fuc <sub>1</sub> Man <sub>3</sub> GlcNAc <sub>4</sub> -2AA	0.47	0.49	-	-	-	0.96	1.58	-	-	-	-	1.58
11		1516.40/1516.28	Man <sub>6</sub> GlcNAc <sub>2</sub> -2AA	17.14	-	-	-	-	17.14	13.60	-	-	-	-	13.60
12		1907.00/1906.85	Gal <sub>2</sub> Fuc <sub>1</sub> Man <sub>3</sub> GlcNAc <sub>4</sub> -2AA	0.43	4.03	4.73	-	-	9.19	0.59	6.10	4.29	-	-	10.98
13		1678.55/1678.39	Man <sub>7</sub> GlcNAc <sub>2</sub> -2AA	11.23	-	-	-	-	11.23	6.29	-	-	-	-	6.29
14		1840.55/1840.51	Man <sub>8</sub> GlcNAc <sub>2</sub> -2AA	8.47	-	-	-	-	8.47	7.05	-	-	-	-	7.05
15		2003.12/2002.98	Man <sub>9</sub> GlcNAc <sub>2</sub> -2AA	6.70	-	-	-	-	6.70	5.36	-	-	-	-	5.36
16		2166.59/2166.66	Gal <sub>2</sub> Man <sub>3</sub> GlcNAc <sub>6</sub> -2AA	0.43	-	-	-	-	0.43	0.17	-	-	-	-	0.17
17		1541.35/1541.48	Gal <sub>1</sub> Fuc <sub>1</sub> Man <sub>3</sub> GlcNAc <sub>3</sub> -2AA	1.48	-	-	-	-	1.48	1.62	-	-	-	-	1.62
18		1703.45/1703.33	Gal <sub>1</sub> Fuc <sub>1</sub> Man <sub>4</sub> GlcNAc <sub>3</sub> -2AA	0.48	-	-	-	-	0.48	-	-	-	-	-	-
19		1598.55/1598.50	Gal <sub>1</sub> Man <sub>3</sub> GlcNAc <sub>4</sub> -2AA	-	-	-	-	-	-	0.93	-	-	-	-	0.93
20		1760.41/1760.34	Gal <sub>2</sub> Man <sub>3</sub> GlcNAc <sub>4</sub> -2AA	-	2.62	1.40	-	-	4.02	-	2.72	1.37	-	-	4.09
21		1719.48/1719.61	Gal <sub>1</sub> Man <sub>3</sub> GlcNAc <sub>3</sub> -2AA	0.42	-	-	-	-	0.42	-	-	-	-	-	-
22		2109.39/2109.28	Gal <sub>2</sub> Fuc <sub>1</sub> Man <sub>3</sub> GlcNAc <sub>5</sub> -2AA	0.32	-	-	-	-	0.32	0.35	-	-	-	-	0.35
23		1865.44/1865.29	Gal <sub>1</sub> Fuc <sub>1</sub> Man <sub>3</sub> GlcNAc <sub>3</sub> -2AA	0.31	-	-	-	-	0.31	0.33	-	-	-	-	0.33
24		2125.39/2125.44	Gal <sub>3</sub> Man <sub>3</sub> GlcNAc <sub>5</sub> -2AA	-	0.24	0.55	0.68	-	1.47	-	0.54	0.71	1.45	-	2.70
25		1881.47/1881.44	Gal <sub>1</sub> Man <sub>6</sub> GlcNAc <sub>3</sub> -2AA	-	0.25	-	-	-	0.25	-	-	-	-	-	-
26		2271.35/2271.45	Gal <sub>3</sub> Fuc <sub>1</sub> Man <sub>3</sub> GlcNAc <sub>5</sub> -2AA	-	0.92	0.49	2.76	-	4.17	-	0.85	0.33	2.42	-	3.60
27		2474.69/2474.53	Gal <sub>3</sub> Fuc <sub>1</sub> Man <sub>3</sub> GlcNAc <sub>6</sub> -2AA	-	-	-	-	-	-	-	0.15	-	-	-	0.15
28		2490.98/2491.02	Gal <sub>4</sub> Man <sub>3</sub> GlcNAc <sub>6</sub> -2AA	-	0.14	-	0.31	-	0.45	-	-	-	0.38	-	0.38
29		2636.44/2636.36	Gal <sub>4</sub> Fuc <sub>1</sub> Man <sub>3</sub> GlcNAc <sub>6</sub> -2AA	-	0.35	0.92	3.44	2.10	6.81	-	0.69	0.60	2.76	2.02	6.07
30		3003.04/3002.59	Gal <sub>5</sub> Fuc <sub>1</sub> Man <sub>3</sub> GlcNAc <sub>7</sub> -2AA	-	0.07	0.32	1.81	0.80	3.00	-	0.06	0.12	0.53	0.14	0.85

Table 1. continued

no.	structure <sup>a</sup>	observed m/z WM266-4/115	monosaccharide composition	relative abundances (%) to total <i>N</i> -glycans <sup>b</sup>											
				WM266-4 cells					sum of (a-e)	WM115 cells					sum of (a-e)
				(a)	(b)	(c)	(d)	(e)		(a)	(b)	(c)	(d)	(e)	
31		3367.02/3366.78	Gal <sub>6</sub> Fuc <sub>1</sub> Man <sub>3</sub> GlcNAc <sub>8</sub> -2AA	-	0.04	0.16	1.18	0.48	1.86	-	-	0.09	0.36	0.06	0.51
32		3732.00/3732.34	Gal <sub>7</sub> Fuc <sub>1</sub> Man <sub>3</sub> GlcNAc <sub>9</sub> -2AA	-	-	0.11	0.87	0.30	1.28	-	-	0.05	0.19	-	0.24
33		4097.92/4098.21	Gal <sub>8</sub> Fuc <sub>1</sub> Man <sub>3</sub> GlcNAc <sub>10</sub> -2AA	-	-	0.07	0.56	0.13	0.76	-	-	0.03	0.09	-	0.12
34		4462.07/4462.34	Gal <sub>9</sub> Fuc <sub>1</sub> Man <sub>3</sub> GlcNAc <sub>11</sub> -2AA	-	-	0.05	0.25	0.04	0.34	-	-	-	-	-	-
35		4827.69/4827.31	Gal <sub>10</sub> Fuc <sub>1</sub> Man <sub>3</sub> GlcNAc <sub>12</sub> -2AA	-	-	0.04	0.14	-	0.18	-	-	-	-	-	-

<sup>a</sup> Structures of *N*-glycans were assigned based on the monosaccharide composition. <sup>b</sup> Relative abundances (%) to total *N*-glycans were calculated as the ratios of individual *N*-glycans observed in five fractions. (a) Asialo-/highmannose-, (b) monosialo-, (c) disialo-, (d) trisialo-, and (e) tetrasialo-fraction. Abbreviations: Gal, galactose; Man, mannose; Fuc, fucose; GlcNAc, N-acetylglucosamine. Symbols: light gray-filled circle, Gal; gray-filled circle, Man; black-filled square, GlcNAc; black-filled triangle, Fuc.

cells were slightly higher than those ( $16.0 \pm 2.8\%$ ) of WM266-4 cells. In contrast, disialo (peak c), trisialo (peak d), and tetrasialo (peak e) *N*-glycans in WM266-4 were present more abundantly than those in WM115 cells.

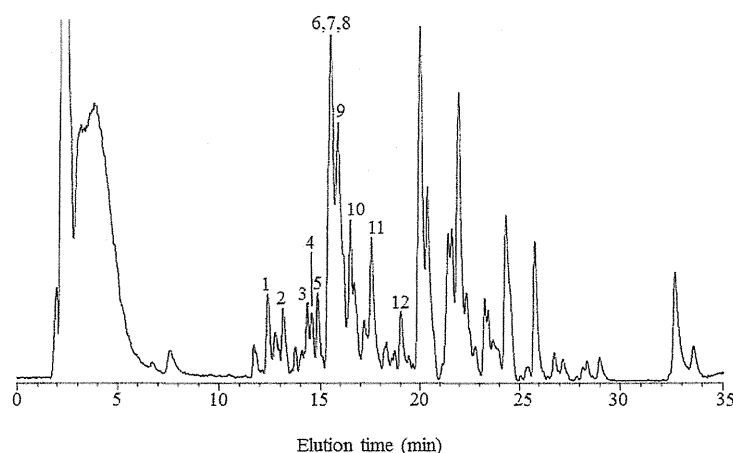
The glycan groups thus separated were further analyzed by NP-HPLC as asialo-*N*-glycans to improve resolutions among peaks. In asialo-/high-mannose fractions, a large amount of high-mannose type *N*-glycans were found as major constituents in both cells (Figure 2). Each peak was collected and analyzed by mass spectrometry and assigned as listed in Table 1.

Peaks 1, 4, 8, 11, 13, 14, and 15 were due to high-mannose type *N*-glycans having 3, 4, 5, 6, 7, 8, and 9 mannose residues. Structures of these *N*-glycans were easily confirmed by comparison with the standard samples obtained from RNase B and by combination of Jackbean  $\alpha$ -mannosidase digestion and MALDI-TOF MS analysis. Elution positions of peaks 8, 11, 13, 14, and 15 were the same with those of five high-mannose-type *N*-glycans (Man<sub>5</sub>, 6, 7, 8, and 9) prepared from RNase B which contains only high-mannose-type glycans. Furthermore, when asialo-/high-mannose fractions (peak a) were digested with Jackbean  $\alpha$ -mannosidase, peaks 1, 4, 8, 11, 13, 14, and 15 completely disappeared. These data clearly indicate that these peaks were due to high-mannose-type *N*-glycans.

After neuraminidase digestion of sialic acid-containing *N*-glycan fractions (peaks b, c, d, and e in Figure 1), the mixture of desialylated *N*-glycans from each fraction was analyzed in the same manner. In monosialo fractions, peaks 12 and 20, which showed molecular ions at  $m/z$  1907.00/1906.85 and 1760.41/1760.34, respectively, were abundantly present in both melanoma cells and are due to monofucosylated diantennary *N*-glycan and diantennary *N*-glycan, respectively. 18, 21, 25, and 28 were observed only in WM266-4 cells, but 19 and 27 were observed only in WM115 cells. In disialo fractions, the major *N*-glycan 12 observed at 24 min showed a molecular ion at  $m/z$  1907.00/1906.85 that was due to monofucosylated diantennary *N*-glycan. 12, 26, and 29 were observed commonly in WM266-4 and WM115 cells and assigned as monofucosylated diantennary, triantennary, and tetraantennary *N*-glycans, respectively. A small amount of tetraantennary *N*-glycans (30, 31, 32, and 33), having one to four additional LacNAc (Gal-GlcNAc) residues, were observed in both melanoma cells as characteristic ladder peaks. In trisialo fractions, triantennary *N*-

glycans (24 and 26) and tetraantennary *N*-glycans (29) were commonly observed in both WM266-4 and WM115 cells. Tetraantennary *N*-glycans derived from WM266-4 cells showed larger amount of ladder peaks (30, 31, 32, and 33) between 30 and 35 min than those in WM115 cells. Also, *N*-glycans (34 and 35) having higher molecular weights were also detected only in WM266-4 cells. These ladder peaks (peaks 30–35) were due to tetraantennary *N*-glycans having different numbers of LacNAc residues. For example, *N*-glycans (34 and 35) showed molecular ions at  $m/z$  4462 and 4827, respectively, and were assigned as tetraantennary *N*-glycans having five and six LacNAc residues at the nonreducing terminal ends (Supporting Information Figure S1). Although *N*-glycans having small numbers of polyLacNAc residues (30, 31, 32, and 33) were also observed in WM115 cells, their relative abundances to total *N*-glycans were significantly lower than those in WM266-4 cells. In tetrasialo fractions, monofucosylated tetraantennary *N*-glycan (29) was the major glycan observed in both cells. Tetraantennary *N*-glycans substituted with multiple poly-lactosamine residues (32, 33, and 34) were observed only in WM266-4 cells.

In summary, we identified 35 *N*-glycans (as asialo *N*-glycans) as shown in Table 1. Most of the complex-type *N*-glycans were commonly observed in both WM266-4 and WM115 cells. Typical complex-type *N*-glycans with one Fuc residue (12, 26, and 29) were abundantly observed in both melanoma cells, and the sum of relative abundances of these glycans in WM266-4/WM115 cells were 9.19%/10.98% (12), 4.17%/3.60% (26), and 6.81%/6.07% (29), respectively. These results indicate that there are no remarkable difference in the biosynthetic machinery for core structure of bi- (12, 20), tri- (24, 26), and tetra-antennary (28, 29) *N*-glycans. In contrast, expression levels of polyLacNAc-carrying *N*-glycans (30, 31, 32, and 33) were significantly higher in WM266-4 cells. The sum of relative abundances of 30 and 31 in WM266-4 were 3.5-fold higher than those in WM115. Also, relative abundances of 32 and 33 were markedly higher in WM266-4 cells. PolyLacNAc-carrying *N*-glycans with additional LacNAc residues (34 and 35) were observed only in WM266-4 cells. Thus, polyLacNAc-carrying *N*-glycans were abundantly expressed in metastatic melanoma cells (WM266-4) as compared with primary melanoma cells (WM115). The expression level of polylactosamine-type *N*-



**Figure 3.** Total ion chromatogram of DSA-bound glycopeptides. Analytical conditions: see Materials and Methods. Peak numbers correspond to those in the list of Table 2

**Table 2.** Glycoproteins Having Polylactosamine-Carrying *N*-Glycans Identified in WM266-4 Cells

peptide no.	protein name	MW (kDa)	precursor ions	error (Da)	score	peptide sequence <sup>a,b</sup>
1	CD63 antigen	25.6	[M + 2H] <sup>2+</sup> = 738.30	0.02	25	CCGAANYTDWEK
2	CD109 antigen	161.7	[M + 2H] <sup>2+</sup> = 706.36	0.02	26	TQDEILFSNSTR
3	cell adhesion molecule 1	48.5	[M + 2H] <sup>2+</sup> = 689.37	0.02	39	VSLT <u>N</u> VSISEGR
4	chondroitin sulfate proteoglycan 4 (CSPG4)	250.5	[M + 2H] <sup>2+</sup> = 644.36	0.01	71	GVNASAVV <u>N</u> VTVR
5	CD59 antigen	14.5	[M + 2H] <sup>2+</sup> = 901.92	0.02	78	TAVN <u>C</u> SSDFDAELITK
6	CD63 antigen	25.6	[M + 2H] <sup>2+</sup> = 707.00	0.07	23	CCGAANYTDWEKIPMSK
7	CD63 antigen	25.6	[M + 2H] <sup>2+</sup> = 852.07	0.03	67	NRVPDSCCINVTGCGINFNEK
8	basigin (CD147)	42.2	[M + 3H] <sup>3+</sup> = 663.35	0.03	50	ILLTCSL <u>N</u> DSATEVTVGR
9	chondroitin sulfate proteoglycan 4 (CSPG4)	250.5	[M + 2H] <sup>2+</sup> = 742.91	0.02	70	LDPTVLDAGELAN <u>R</u>
10	lysosome-associated membrane glycoprotein-1	44.9	[M + 3H] <sup>3+</sup> = 721.71	0.03	62	SGPKNMFTDLPDATVVL <u>N</u> R
11	lysosome-associated membrane glycoprotein-1	44.9	[M + 2H] <sup>2+</sup> = 897.97	0.02	34	<u>N</u> MTFDLPDATVVL <u>N</u> R
12	chondroitin sulfate proteoglycan 4 (CSPG4)	250.5	[M + 3H] <sup>3+</sup> = 897.09	0.06	40	YVHDGSETLTDSPVLMANASEMDR

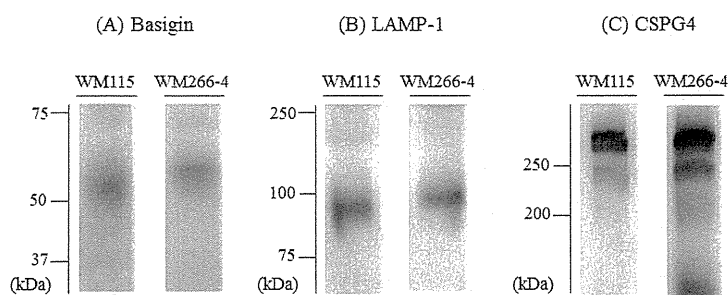
<sup>a</sup>Sequences marked with underline are by the *N*-glycosylation potential sites (Asn-X-Ser/Thr). <sup>b</sup>All cysteine residues are modified with carbamidomethylation.

glycans may be correlated with expression level of  $\beta$ 1-6*N*-acetyl-glucosamine ( $\beta$ 1-6GlcNAc), and  $\beta$ 1-6 GlcNAc branching on *N*-glycans is increased in malignant transformation in cancer metastasis.<sup>23–25</sup> Some groups reported *N*-glycosylation patterns in human melanoma cells at different progression stages by lectin-blotting analysis using *Phaseolus vulgaris*-leucoagglutinin (PHA-L) which recognizes  $\beta$ 1-6GlcNAc branch on Man $\alpha$ 1-6 branch of *N*-glycans and demonstrated that  $\beta$ 1-6GlcNAc-expressing glycoproteins were abundantly observed in metastatic melanoma cells (e.g., WM239, WM9, and A375).<sup>26,27</sup> It is well-known that *N*-acetylglucosaminyltransferase-V (GnT-V, *Mgat5*) catalyzes the transfer of GlcNAc to the OH-6 position of the Man residue in Man $\alpha$ 1-6Man branch of trimannosyl core structure and higher expression of this enzyme has been shown to induce metastatic spread.<sup>24</sup> Difference in expression level of polylactosamine-type *N*-glycans may be due to the difference in expression level of GnT-V between both cells. These data prompted us to find specific protein(s) expressing *N*-glycans having multiple polylactosamine-type residues that were observed in WM266-4.

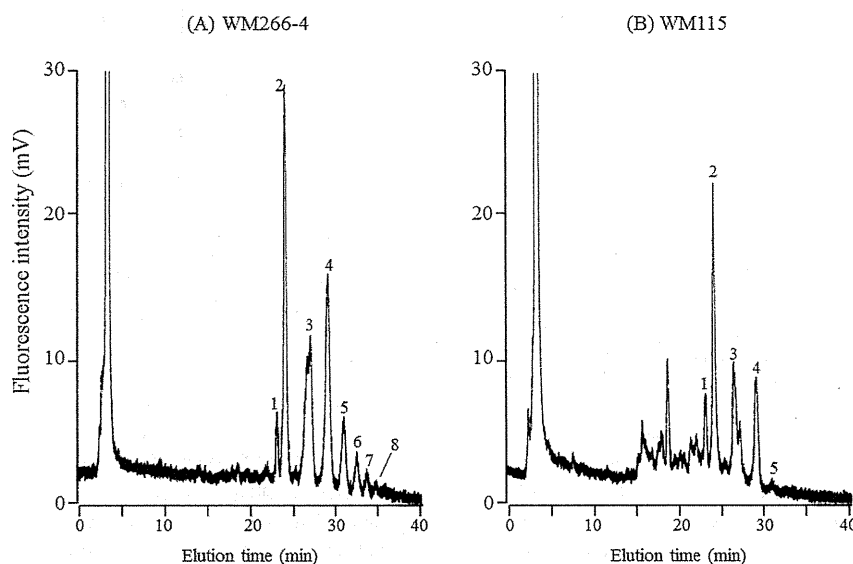
#### Identification of Glycoproteins Carrying PolyLacNAc Residues in WM266-4 Cells

We previously found that integrin- $\alpha$ 5 (CD49e), carcinoembryonic antigen (CEA)-related cell adhesion molecule 5 (CD66e), CD107a, and CD107b were common glycoproteins carrying polyLacNAc-type *N*-glycans in histiocytic lymphoma cells (U937) and gastric cancer cells (MKN45).<sup>18</sup> These glycoproteins were confirmed as follows: (i) capturing of glycopeptides by characteristic glycan-recognizing lectin(s), (ii) analysis of the released glycans from the captured glycopeptides after *N*-glycoamidase F, and (iii) LC/MS of the peptides having *N*-glycosylation sites.

In the similar manner employed in the previous studies, whole protein from WM266-4 cells was digested with TPCK-trypsin, and polyLacNAc-carrying glycopeptides were collected using a *Datura stramonium* agglutinin (DSA)-immobilized agarose column<sup>18</sup> (Supporting Information Figure S2 and Table S1). It is known that DSA shows specificity to  $\beta$ 1–4 linked oligomers of GlcNAc and also shows affinity to polyLacNAc residues on glycoconjugates.<sup>18</sup> The collected DSA-bound glycopeptides were digested with *N*-glycoamidase F, and the mixtures of peptides after releasing *N*-glycans thus obtained were analyzed by LCMS (Figure 3). More than 30 peaks were observed on the total ion chromatogram. The peaks



**Figure 4.** Western blot analysis of glycoproteins containing polyLacNAc residues commonly present in WM266-4 and WM115 cells. Analytical conditions: separation gel, 10% T/2.6% C; blotting buffer, 48 mM Tris-39 mM glycine-20% methanol; blocking buffer for lectin blot, 0.05% Tween 20 in PBS; blocking buffer for Western blot, 5% skim milk-0.05% Tween 20 in PBS. Detection: HRP-DAB.



**Figure 5.** Analysis of *N*-glycans expressed on CSPG4 in WM266-4 (A) and WM115 (B) cells. The *N*-glycans were previously digested with neuraminidase. Analytical conditions are the same as in Figure 2. The *m/z* values and structures of individual peaks were summarized in Table 3. Structures corresponding to the peak numbers are summarized in Table 3

observed from 11 to 19 min showed molecular ions from *m/z* 500 to *m/z* 1000 (charge state: +2 or +3) (Supporting Information Table S2). On the other hand, peaks appeared later than 20 min showed low molecular ions (less than *m/z* 500). The small peptides have little information on peptide sequences. Therefore, the peaks observed from 11 to 19 min were analyzed by MS/MS technique, and 12 peptides were proved to have Asn-X-Ser/Thr consensus sequence for *N*-glycosylation site as shown in Table 2 (Supporting Information Figure S3, Table S2, and Table S3).

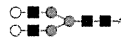
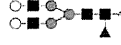
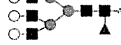
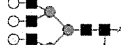

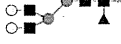
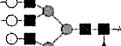
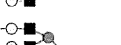
The sequences of CCGAANYTDWEK (1), CCGAANYTDWEKIPSMK (6), and NRPVDSCCINVTGCGINFNEK (7) were assigned to the sequences of CD63 (CD63\_HUMAN:P08962). The presence of polyLacNAc-type *N*-glycans in CD63 of human melanoma cells was already reported.<sup>28</sup> Three peptide sequences (4, 9, and 12 for GVNASAVVNVTVR, LDPTVLDAGELANR, and YVHDGSETLTDSFVLMANASEMDR, respectively) were due to chondroitin sulfate proteoglycan 4 (CSPG4\_HUMAN:Q6UVK1). CSPG4 is a high molecular weight glycoprotein having both *N*-glycans and CS chains, although the presence of polyLacNAc-type *N*-glycans in CSPG4 has not been reported.

Peptides 10 (SGPKNMTFDLPSDATVVLNR) and 11 (NMTFDLPSDATVVLNR) corresponded to the sequences for lysosome-associated membrane glycoprotein-1 (LAMP1\_HUMAN:P11279). *N*-Glycans on LAMP-1 in various cells are often modified with polyLacNAc.<sup>29–31</sup> We also reported that LAMP-1 in some cancer cells contained a large amount of *N*-glycans having polyLacNAc.<sup>18</sup> Basigin (BASI\_HUMAN:P35613) as well as LAMP-1 are glycoproteins having polyLacNAc-type *N*-glycans.<sup>29–31</sup> Krishnan et al. also reported that the immunoprecipitated LAMP-1 from the cell lysates of mouse high metastatic melanoma cells (B16F10) express higher levels of polyLacNAc-type glycans than those of low metastatic melanoma cells (B16F1).<sup>32</sup> The results are well consistent with our present findings. Other sequences (2, 3, and 5) were due to CD109 (CD109\_HUMAN:Q6YHK3), cell adhesion molecule 1 (CADM1\_HUMAN:Q9BY67), and CD59 (CD59\_HUMAN:P13987), respectively.

These proteins having polyLacNAc-type-*N*-glycans were further confirmed by Western blot analysis (Figure 4).

Basigin was detected at 50–60 kDa (Figure 4A) in both cells. LAMP-1 is composed of 417 amino acids and observed at ca. 100 kDa (Figure 4B) also in both cells. LAMP-1 is a highly

Table 3. List of *N*-Glycans Observed in CSPG4 Derived from WM266-4 and WM115 Cells<sup>a</sup>

peak no.	observed m/z		monosaccharide composition	structure	relative abundances <sup>b</sup> (mean ± SD; n=3)	
	WM266-4	WM115			WM266-4	WM115
1	1760.70	1761.15	Gal <sub>2</sub> Man <sub>3</sub> GlcNAc <sub>4</sub> -2AA		10.3±4.6%	11.9±1.1%
2	1907.21	1907.26	Gal <sub>2</sub> Fuc <sub>1</sub> Man <sub>3</sub> GlcNAc <sub>4</sub> -2AA		38.7±1.0%	47.7±3.5%
3	2272.27	2272.19	Gal <sub>3</sub> Fuc <sub>1</sub> Man <sub>3</sub> GlcNAc <sub>5</sub> -2AA		14.3±4.9%	19.8±0.7%
4	2637.59	2637.14	Gal <sub>4</sub> Fuc <sub>1</sub> Man <sub>3</sub> GlcNAc <sub>6</sub> -2AA		20.8±2.6%	18.5±3.2%
5	3002.75	3003.25	Gal <sub>5</sub> Fuc <sub>1</sub> Man <sub>3</sub> GlcNAc <sub>7</sub> -2AA		7.4±1.4%	2.1±1.3%
6	3367.85	n.d. <sup>c</sup>	Gal <sub>6</sub> Fuc <sub>1</sub> Man <sub>3</sub> GlcNAc <sub>8</sub> -2AA		4.2±2.3%	-
7	3733.25	n.d. <sup>c</sup>	Gal <sub>7</sub> Fuc <sub>1</sub> Man <sub>3</sub> GlcNAc <sub>9</sub> -2AA		3.0±2.8%	-
8	4098.56	n.d. <sup>c</sup>	Gal <sub>8</sub> Fuc <sub>1</sub> Man <sub>3</sub> GlcNAc <sub>10</sub> -2AA		1.3±1.0%	-

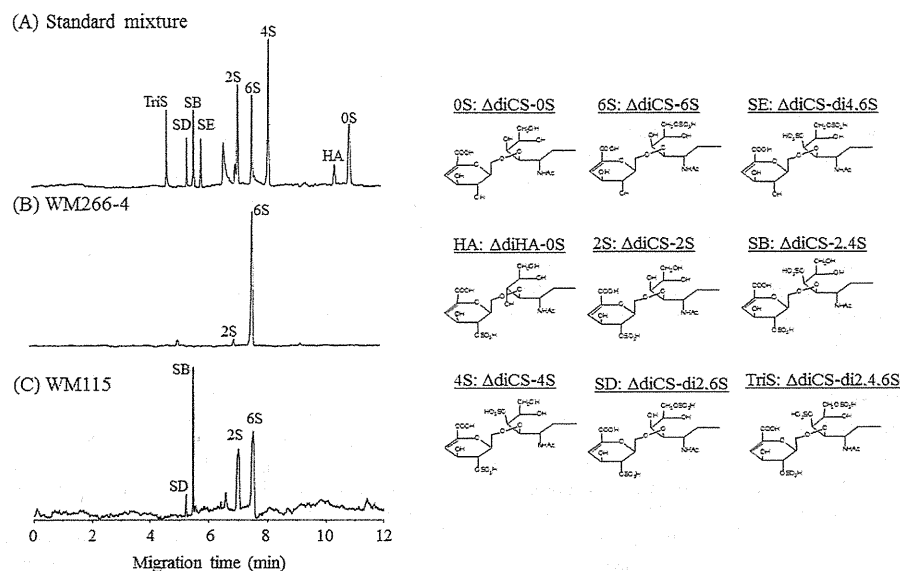
<sup>a</sup>Abbreviations: Gal, galactose; Man, mannose; Fuc, fucose; GlcNAc, *N*-acetylglucosamine. Symbols: light gray-filled circle, Gal; gray-filled circle, Man; black-filled square, GlcNAc; black-filled triangle, Fuc. <sup>b</sup>Relative abundances were calculated as ratios of individual *N*-glycans to total *N*-glycans expressed in CSPG4. <sup>c</sup>Not detected.

glycosylated protein, having 18 *N*-glycosylation sites and also 4 *O*-glycosylation sites.<sup>33</sup> Basigin and LAMP-1 in WM266-4 cells showed slightly larger molecular sizes than those in WM115 cells. The difference in molecular sizes of these glycoproteins may be due to molecular sizes of attached *N*-glycans because polyLacNAc-type *N*-glycans are more abundantly expressed in WM266-4 cells as shown in Table 1. CSPG4 was observed at >250 kDa (Figure 4C). Although core protein of CSPG4 is composed of 2322 amino acids, the observed large molecular size is due to the presence of 15 *N*-glycans and a chondroitin sulfate (CS) chain.<sup>34</sup> CD63, of which presence was confirmed by LC/MS, could not be detected in WM115 cells by Western blot analysis (data not shown). Among these glycoproteins commonly observed in WM266-4 and WM115 cells, CSPG4 in melanoma cells has been reported to be a melanoma specific antigen.<sup>35</sup> CS chains in CSPG4 molecule are involved in various biological functions such as cell adhesion, cell invasion, and cell angiogenesis.<sup>36–38</sup> Fukushi et al. reported that CSPG4 promotes cell motility and angiogenesis via interaction with galectin-3 which is the endogenous polyLacNAc-binding protein.<sup>38</sup> CS chains on CSPG4 regulate matrix metalloproteinase (MMP)-dependent human melanoma invasion.<sup>39</sup> Thus, changes in glycosylation during malignant transformation and tumor progression (i.e., difference in glycan profiles between WM115 cells and WM266-4 cells) should have some correlation with physiological states of these cells. However, detailed information on structures of *N*-glycans and chondroitin sulfate attached to the core protein of CSPG4 is not available.

#### *N*-Glycans of CSPG4 Obtained from WM266-4 and WM115 Cells by Immunoprecipitation Method

As shown in Figure 5, both cells showed similar *N*-glycan profiles. However, relative abundances of *N*-glycans were significantly different between WM266-4 and WM115 cells.

CSPG4 expressed in WM266-4 cells contained a large amount of polyLacNAc-type *N*-glycans (15.9% for peaks 5, 6, 7, and 8), and the relative abundance was ca. 7.5-fold higher than that of WM115 cells. In WM115 cells, typical complex-type *N*-glycans (i.e., biantennary (1 and 2)-, triantennary (3)-, and tetraantennary (4)-glycans) were observed as the major glycans. The sum of these typical complex-type *N*-glycans (1–4) was 97.9% in total *N*-glycans, and the relative abundance of polyLacNAc-type *N*-glycans was very low (2.1%). Oncogene activation often stimulates expression of the Golgi enzymes that are responsible for the synthesis of polyLacNAc-type *N*-glycans.<sup>40,41</sup> PolyLacNAc-type *N*-glycans, which are found on proteins such as growth factor receptors and integrins, are shown to enhance growth signaling in motile tumor cells.<sup>42</sup> It was also reported that polyLacNAc-type *N*-glycan levels were increased in highly metastatic tumor cell lines.<sup>32,43</sup> Krishnan et al. investigated the biological roles of polyLacNAc residues on organ specific metastasis and revealed that high metastatic melanoma cell, expressing high level of polyLacNAc-*N*-glycans, show high affinity to the galectin-3-expressed lung vascular endothelium.<sup>32</sup> The increased level of polyLacNAc-type *N*-glycans may change cell adhesion through carbohydrate–lectin interaction, resulting in facilitating tumor cell invasion and metastasis.<sup>44</sup> The present data, which show higher expression of polyLacNAc-type *N*-glycans in metastatic WM266-4 cells, support these previously reported results.



**Figure 6.** Analysis of unsaturated disaccharides expressed on CSPG4 in WM266-4 and WM115 cells and structures of unsaturated disaccharides from chondroitin sulfate/hyaluronic acid. (A) standard mixture of nine unsaturated disaccharides. (B and C) Results on digestion of CSPG4 with chondroitinase ABC. Analytical conditions: capillary, fused silica capillary (50  $\mu\text{m}$  i.d., 30 cm); running buffer, 0.1 M Tris-phosphate buffer (pH 3.0); applied voltage,  $-25$  kV; injection, pressure injection (1.0 psi, 5s); temperature,  $25$   $^{\circ}\text{C}$ ; detection, He-Cd laser-induced fluorescent detection (excitation 325 nm, emission 405 nm).

#### Analysis of Chondroitin Sulfate of CSPG4 Obtained from WM266-4 and WM115 Cells

Alterations in sulfation pattern of CS chains have been reported in relation to malignant transformation and progression.<sup>45–47</sup> Human gastric carcinoma-derived versican, which is a high molecular weight chondroitin sulfate proteoglycan, showed increase of 6-sulfated CS chains with parallel decrease of 4-sulfated CS chains as compared to human normal gastric mucosa.<sup>46</sup> Iida et al. reported that chondroitin 4-sulfate expressed on melanoma cells activated matrix metalloproteinase-2 (MMP-2) and enhanced cell invasion and metastasis.<sup>48</sup>

We performed comparative analysis of CS chains on CSPG4 derived from WM266-4 and WM115 cells. Another portion of CSPG4 used for the analysis of *N*-glycans as described above was digested with chondroitinase ABC, and the eliminated unsaturated disaccharides was labeled with 2-AA<sup>22</sup> and analyzed by laser-induced fluorescence detection (LIF)-CE (Figure 6).

WM266-4 cells showed simple profiles and contained  $\Delta\text{diCS-6S}$  (6S) as the major component and  $\Delta\text{diCS-2S}$  (2S) as the minor one. Disulfated unsaturated disaccharides such as SD, SE, and SB were not detected. In contrast, four unsaturated disaccharides,  $\Delta\text{diCS-2S}$  (2S),  $\Delta\text{diCS-6S}$  (6S),  $\Delta\text{diCS-di2.4S}$  (SB), and  $\Delta\text{diCS-di2.6S}$  (SD), were observed in WM115 cells. Disulfated unsaturated disaccharides (SB and SD), which are abundantly present in dermatan sulfate (DS), were observed only in WM115 cells. It should be noticed that  $\Delta\text{diCS-4S}$  (4S) given from chondroitin 4-sulfate (CS4) was not detected in both melanoma cells. Iida et al. reported that CSPG4 is decorated with CS4 in human melanoma.<sup>48</sup> Our present data are quite different, with their report indicating that CS4 is the major component of CSPG4 in melanoma cell lines.<sup>48–50</sup> CS chains on CSPG4 is believed to be important for their biological functions such as activation of matrix metalloproteinase, activation of integrin, or cell surface localization.<sup>37,48,51</sup> Recent studies have also reported that CSPG4 enhanced

activation of integrin-related signal transduction pathways, which may be an important role on tumor progression.<sup>52,53</sup> Although how or whether tumor-associated changes in the sulfation patterns (e.g., chondroitin-6-sulfation) and CS chain extension on CSPG4 occur is currently unknown, metastasis-associated changes in CS modification on CSPG4 may facilitate migration and invasion.

#### CONCLUSION

In the present study, we performed comparative analysis of glycoproteins expressed commonly in the matched patient primary and metastatic melanoma cell lines. Although most of the complex-type *N*-glycans were commonly observed in both primary and metastatic melanoma cells (WM115 and WM266-4 cells, respectively), expression level of polyLacNAc-carrying *N*-glycans was significantly higher in WM266-4 cells, and we found that expression of polyLacNAc-carrying *N*-glycans was preferentially due to LAMP-1, CD63, Basigin, and CSPG4 as examined by a combination of lectin affinity chromatography and LC/MS-based proteomics approaches. Among the identified glycoproteins, CSPG4 is a well-known marker for melanoma, and we found that the expression level of polyLacNAc-carrying *N*-glycans in metastatic melanoma (WM266-4) was significantly higher than those in primary melanoma (WM115). The results are in good agreement with the reports describing that polyLacNAc-carrying *N*-glycans are increased in malignant transformation in cancer metastasis.<sup>23–27</sup>

Sulfation patterns of chondroitin sulfate chain in CSPG4 showed distinct changes between primary and metastatic melanoma cells. In WM266-4 cells,  $\Delta\text{diCS-6S}$  (6S) was the major component. In contrast, WM115 showed relatively complex unsaturated disaccharide profiles, and four unsaturated disaccharides,  $\Delta\text{diCS-2S}$  (2S),  $\Delta\text{diCS-6S}$  (6S),  $\Delta\text{diCS-di2.4S}$  (SB), and  $\Delta\text{diCS-di2.6S}$  (SD) as the major components, were

observed in WM115 cells. It should be noticed that the present results were inconsistent with the previous reports that CSPG4 was mainly decorated with chondroitin 4-sulfate in human melanomas.<sup>48,49</sup>

In conclusion, post-translational modification of a protein with carbohydrates in melanoma cells becomes quite different with malignant transformation in acquiring metastasis ability, and glycans attached to tumor-specific cells are distinctively different with changes of their physiological state such as metastasis ability. Although further studies are required, comparative analyses of glycans attached to disease-specific glycoproteins will lead to develop new markers for determination of the degree of malignancy.

## ■ ASSOCIATED CONTENT

### Supporting Information

MS/MS spectra of polyLacNAc-type N-glycans observed in WM266-4 cells, NP-HPLC analysis of N-glycan on glycopeptides fractionated by DSA-agarose column, MSMS spectra of deglycosylated peptides captured by DSA-agarose (PDF); summary of N-glycans on glycopeptides fractionated by DSA-agarose column, summary of MS analysis of deglycosylated peptides captured by DSA-agarose column, summary of MSMS analysis of glycopeptides captured by DSA-agarose column (XLSX). This material is available free of charge via the Internet at <http://pubs.acs.org>.

## ■ AUTHOR INFORMATION

### Corresponding Author

\*Phone: +80-6-6730-5880 ext 3868. Fax: +80-6-6730-1394. E-mail: [k\\_kakehi@phar.kindai.ac.jp](mailto:k_kakehi@phar.kindai.ac.jp).

### Notes

The authors declare no competing financial interest.

## ■ REFERENCES

- Helenius, A.; Aebi, M. Intracellular functions of N-linked glycans. *Science* **2001**, *291* (5512), 2364–2369.
- Parodi, A. J. Protein glucosylation and its role in protein folding. *Annu. Rev. Biochem.* **2000**, *69*, 69–93.
- Angata, T.; Fujinawa, R.; Kurimoto, A.; Nakajima, K.; Kato, M.; Takamatsu, S.; Korekane, H.; Gao, C. X.; Ohtsubo, K.; Kitazume, S.; Taniguchi, N. Integrated approach toward the discovery of glyco-biomarkers of inflammation-related diseases. *Ann. N. Y. Acad. Sci.* **2012**, *1253*, 159–169.
- Drake, P. M.; Cho, W.; Li, B.; Prakobphol, A.; Johansen, E.; Anderson, N. L.; Regnier, F. E.; Gibson, B. W.; Fisher, S. J. Sweetening the pot: adding glycosylation to the biomarker discovery equation. *Clin. Chem.* **2009**, *56* (2), 223–236.
- Fuster, M. M.; Esko, J. D. The sweet and sour of cancer: glycans as novel therapeutic targets. *Nature Rev. Cancer* **2005**, *5* (7), 526–542.
- Narimatsu, H.; Sawaki, H.; Kuno, A.; Kaji, H.; Ito, H.; Ikehara, Y. A strategy for discovery of cancer glyco-biomarkers in serum using newly developed technologies for glycoproteomics. *FEBS J.* **2009**, *277* (1), 95–105.
- Tharmalingam, T.; Marino, K.; Rudd, P. M. Platform technology to identify potential disease markers and establish heritability and environmental determinants of the human serum N-glycome. *Carbohydr. Res.* **2010**, *345* (10), 1280–1282.
- Kannagi, R.; Fukushi, Y.; Tachikawa, T.; Noda, A.; Shin, S.; Shigeta, K.; Hiraiwa, N.; Fukuda, Y.; Inamoto, T.; Hakomori, S.; et al. Quantitative and qualitative characterization of human cancer-associated serum glycoprotein antigens expressing fucosyl or sialyl-fucosyl type 2 chain polylectosamine. *Cancer Res.* **1986**, *46* (5), 2619–2626.
- Korczak, B.; Goss, P.; Fernandez, B.; Baker, M.; Dennis, J. W. Branching N-linked oligosaccharides in breast cancer. *Adv. Exp. Med. Biol.* **1994**, *353*, 95–104.
- Miyake, M.; Kohno, N.; Nudelman, E. D.; Hakomori, S. Human IgG3 monoclonal antibody directed to an unbranched repeating type 2 chain (Gal beta 1—4GlcNAc beta 1—3Gal beta 1—4GlcNAc beta 1—3Gal beta 1—R) which is highly expressed in colonic and hepatocellular carcinoma. *Cancer Res.* **1989**, *49* (20), 5689–5695.
- Zenita, K.; Kirihata, Y.; Kitahara, A.; Shigeta, K.; Higuchi, K.; Hirashima, K.; Murachi, T.; Miyake, M.; Takeda, T.; Kannagi, R. Fucosylated type-2 chain polylectosamine antigens in human lung cancer. *Int. J. Cancer* **1988**, *41* (3), 344–349.
- Sozzani, P.; Arisio, R.; Porpiglia, M.; Benedetto, C. Is Sialyl Lewis x antigen expression a prognostic factor in patients with breast cancer? *Int. J. Surg. Pathol.* **2008**, *16* (4), 365–374.
- Arnold, J. N.; Saldova, R.; Hamid, U. M.; Rudd, P. M. Evaluation of the serum N-linked glycome for the diagnosis of cancer and chronic inflammation. *Proteomics* **2008**, *8* (16), 3284–3293.
- Kim, Y. S.; Yoo, H. S.; Ko, J. H. Implication of aberrant glycosylation in cancer and use of lectin for cancer biomarker discovery. *Protein Pept. Lett.* **2009**, *16* (5), 499–507.
- Kuno, A.; Ikehara, Y.; Tanaka, Y.; Angata, T.; Unno, S.; Sogabe, M.; Ozaki, H.; Ito, K.; Hirabayashi, J.; Mizokami, M.; Narimatsu, H. Multilectin assay for detecting fibrosis-specific glyco-alteration by means of lectin microarray. *Clin. Chem.* **2011**, *57* (1), 48–56.
- Naka, R.; Kamoda, S.; Ishizuka, A.; Kinoshita, M.; Kakehi, K. Analysis of total N-glycans in cell membrane fractions of cancer cells using a combination of serotonin affinity chromatography and normal phase chromatography. *J. Proteome Res.* **2006**, *5* (1), 88–97.
- Yamada, K.; Kinoshita, M.; Hayakawa, T.; Nakaya, S.; Kakehi, K. Comparative studies on the structural features of O-glycans between leukemia and epithelial cell lines. *J. Proteome Res.* **2009**, *8* (2), 521–537.
- Mitsui, Y.; Yamada, K.; Hara, S.; Kinoshita, M.; Hayakawa, T.; Kakehi, K. Comparative studies on glycoproteins expressing polylectosamine-type N-glycans in cancer cells. *J. Pharm. Biomed. Anal.* **2012**, *70*, 718–726.
- Dickson, P. V.; Gershenwald, J. E. Staging and prognosis of cutaneous melanoma. *Surg. Oncol. Clin. N. Am.* **2011**, *20* (1), 1–17.
- Brochez, L.; Naeyaert, J. M. Serological markers for melanoma. *Br. J. Dermatol.* **2000**, *143* (2), 256–268.
- Kamoda, S.; Nakanishi, Y.; Kinoshita, M.; Ishikawa, R.; Kakehi, K. Analysis of glycoprotein-derived oligosaccharides in glycoproteins detected on two-dimensional gel by capillary electrophoresis using on-line concentration method. *J. Chromatogr., A* **2006**, *1106* (1–2), 67–74.
- Yamada, K.; Mitsui, Y.; Kakoi, N.; Kinoshita, M.; Hayakawa, T.; Kakehi, K. One-pot characterization of cancer cells by the analysis of mucin-type glycans and glycosaminoglycans. *Anal. Biochem.* **2012**, *421* (2), 595–606.
- Datti, A.; Donovan, R. S.; Korczak, B.; Dennis, J. W. A homogeneous cell-based assay to identify N-linked carbohydrate processing inhibitors. *Anal. Biochem.* **2000**, *280* (1), 137–142.
- Dennis, J. W.; Granovsky, M.; Warren, C. E. Glycoprotein glycosylation and cancer progression. *Biochim. Biophys. Acta* **1999**, *1473* (1), 21–34.
- Prokoshyn, N. L.; Puzon-McLaughlin, W.; Takada, Y.; Laferte, S. Integrin alpha3beta1 expressed by human colon cancer cells is a major carrier of oncodevelopmental carbohydrate epitopes. *J. Cell. Biochem.* **1999**, *72* (2), 189–209.
- Ciolkczyk-Wierzbicka, D.; Gil, D.; Hoja-Lukowicz, D.; Litynska, A.; Laidler, P. Carbohydrate moieties of N-cadherin from human melanoma cell lines. *Acta Biochim. Pol.* **2002**, *49* (4), 991–998.
- Przybylo, M.; Martuszevska, D.; Pochec, E.; Hoja-Lukowicz, D.; Litynska, A. Identification of proteins bearing beta1–6 branched N-glycans in human melanoma cell lines from different progression stages by tandem mass spectrometry analysis. *Biochim. Biophys. Acta* **2007**, *1770* (9), 1427–1435.



- (28) Engering, A.; Kuhn, L.; Fluitsma, D.; Hoefsmit, E.; Pieters, J. Differential post-translational modification of CD63 molecules during maturation of human dendritic cells. *Eur. J. Biochem.* **2003**, *270* (11), 2412–2420.
- (29) Carlsson, S. R.; Fukuda, M. The polylectosaminoglycans of human lysosomal membrane glycoproteins lamp-1 and lamp-2. Localization on the peptide backbones. *J. Biol. Chem.* **1990**, *265* (33), 20488–20495.
- (30) Laferte, S.; Dennis, J. W. Purification of two glycoproteins expressing beta 1–6 branched Asn-linked oligosaccharides from metastatic tumour cells. *Biochem. J.* **1989**, *259* (2), 569–576.
- (31) Tang, W.; Chang, S. B.; Hemler, M. E. Links between CD147 function, glycosylation, and caveolin-1. *Mol. Biol. Cell* **2004**, *15* (9), 4043–4050.
- (32) Krishnan, V.; Bane, S. M.; Kawle, P. D.; Naresh, K. N.; Kalraiya, R. D. Altered melanoma cell surface glycosylation mediates organ specific adhesion and metastasis via lectin receptors on the lung vascular endothelium. *Clin. Exp. Metastasis* **2005**, *22* (1), 11–24.
- (33) Carlsson, S. R.; Lycksell, P. O.; Fukuda, M. Assignment of O-glycan attachment sites to the hinge-like regions of human lysosomal membrane glycoproteins lamp-1 and lamp-2. *Arch. Biochem. Biophys.* **1993**, *304* (1), 65–73.
- (34) Hubbard, S. C.; Ivatt, R. J. Synthesis and processing of asparagine-linked oligosaccharides. *Annu. Rev. Biochem.* **1981**, *50*, 555–583.
- (35) Pluschke, G.; Vanek, M.; Evans, A.; Dittmar, T.; Schmid, P.; Itin, P.; Filardo, E. J.; Reisfeld, R. A. Molecular cloning of a human melanoma-associated chondroitin sulfate proteoglycan. *Proc. Natl. Acad. Sci. U. S. A.* **1996**, *93* (18), 9710–9715.
- (36) Eisenmann, K. M.; McCarthy, J. B.; Simpson, M. A.; Keely, P. J.; Guan, J. L.; Tachibana, K.; Lim, L.; Manser, E.; Furcht, L. T.; Iida, J. Melanoma chondroitin sulphate proteoglycan regulates cell spreading through Cdc42, Ack-1 and p130cas. *Nature Cell Biol.* **1999**, *1* (8), 507–513.
- (37) Iida, J.; Meijne, A. M.; Oegema, T. R., Jr.; Yednock, T. A.; Kovach, N. L.; Furcht, L. T.; McCarthy, J. B. A role of chondroitin sulfate glycosaminoglycan binding site in alpha4beta1 integrin-mediated melanoma cell adhesion. *J. Biol. Chem.* **1998**, *273* (10), 5955–5962.
- (38) Fukushi, J.; Makagiansar, I. T.; Stallcup, W. B. NG2 proteoglycan promotes endothelial cell motility and angiogenesis via engagement of galectin-3 and alpha3beta1 integrin. *Mol. Biol. Cell* **2004**, *15* (8), 3580–3590.
- (39) Iida, J.; Pei, D.; Kang, T.; Simpson, M. A.; Herlyn, M.; Furcht, L. T.; McCarthy, J. B. Melanoma chondroitin sulfate proteoglycan regulates matrix metalloproteinase-dependent human melanoma invasion into type I collagen. *J. Biol. Chem.* **2001**, *276* (22), 18786–18794.
- (40) Dennis, J. W.; Kosh, K.; Bryce, D. M.; Breitman, M. L. Oncogenes conferring metastatic potential induce increased branching of Asn-linked oligosaccharides in rat2 fibroblasts. *Oncogene* **1989**, *4* (7), 853–860.
- (41) Dennis, J. W.; Laferte, S.; Waghorne, C.; Breitman, M. L.; Kerbel, R. S. Beta 1–6 branching of Asn-linked oligosaccharides is directly associated with metastasis. *Science* **1987**, *236* (4801), 582–585.
- (42) Beheshti Zavareh, R.; Lau, K. S.; Hurren, R.; Datti, A.; Ashline, D. J.; Gronda, M.; Cheung, P.; Simpson, C. D.; Liu, W.; Wasylshen, A. R.; Boutros, P. C.; Shi, H.; Vengopal, A.; Jurisica, I.; Penn, L. Z.; Reinhold, V. N.; Ezzat, S.; Wrana, J.; Rose, D. R.; Schachter, H.; Dennis, J. W.; Schimmer, A. D. Inhibition of the sodium/potassium ATPase impairs N-glycan expression and function. *Cancer Res.* **2008**, *68* (16), 6688–6697.
- (43) Gu, J.; Sato, Y.; Kariya, Y.; Isaji, T.; Taniguchi, N.; Fukuda, T. A mutual regulation between cell-cell adhesion and N-glycosylation: implication of the bisecting GlcNAc for biological functions. *J. Proteome Res.* **2009**, *8* (2), 431–435.
- (44) Demetriou, M.; Nabi, I. R.; Coppolino, M.; Dedhar, S.; Dennis, J. W. Reduced contact-inhibition and substratum adhesion in epithelial cells expressing GlcNAc-transferase V. *J. Cell Biol.* **1995**, *130* (2), 383–392.
- (45) Theocharis, A. D.; Tsara, M. E.; Papageorgakopoulou, N.; Karavias, D. D.; Theocharis, D. A. Pancreatic carcinoma is characterized by elevated content of hyaluronan and chondroitin sulfate with altered disaccharide composition. *Biochim. Biophys. Acta* **2000**, *1502* (2), 201–206.
- (46) Theocharis, A. D.; Vynios, D. H.; Papageorgakopoulou, N.; Skandalis, S. S.; Theocharis, D. A. Altered content composition and structure of glycosaminoglycans and proteoglycans in gastric carcinoma. *Int. J. Biochem. Cell Biol.* **2003**, *35* (3), 376–390.
- (47) Tsara, M. E.; Papageorgakopoulou, N.; Karavias, D. D.; Theocharis, D. A. Distribution and changes of glycosaminoglycans in neoplasias of rectum. *Anticancer Res.* **1995**, *15* (5B), 2107–2112.
- (48) Iida, J.; Wilhelmson, K. L.; Ng, J.; Lee, P.; Morrison, C.; Tam, E.; Overall, C. M.; McCarthy, J. B. Cell surface chondroitin sulfate glycosaminoglycan in melanoma: role in the activation of pro-MMP-2 (pro-gelatinase A). *Biochem. J.* **2007**, *403* (3), 553–563.
- (49) Price, M. A.; Colvin Wanshura, L. E.; Yang, J.; Carlson, J.; Xiang, B.; Li, G.; Ferrone, S.; Dudek, A. Z.; Turley, E. A.; McCarthy, J. B. CSPG4, a potential therapeutic target, facilitates malignant progression of melanoma. *Pigm. Cell Melanoma Res.* **2011**, *24* (6), 1148–1157.
- (50) Bhavanandan, V. P. Glycosaminoglycans of cultured human fetal uveal melanocytes and comparison with those produced by cultured human melanoma cells. *Biochemistry* **1981**, *20* (19), 5595–5602.
- (51) Stallcup, W. B.; Dahlin-Huppe, K. Chondroitin sulfate and cytoplasmic domain-dependent membrane targeting of the NG2 proteoglycan promotes retraction fiber formation and cell polarization. *J. Cell. Sci.* **2001**, *114* (Pt 12), 2315–2325.
- (52) Chekenya, M.; Krakstad, C.; Svendsen, A.; Netland, I. A.; Staalesen, V.; Tysnes, B. B.; Selheim, F.; Wang, J.; Sakariassen, P. O.; Sandal, T.; Lonning, P. E.; Flatmark, T.; Enger, P. O.; Bjerkvig, R.; Sioud, M.; Stallcup, W. B. The progenitor cell marker NG2/MPG promotes chemoresistance by activation of integrin-dependent PI3K/Akt signaling. *Oncogene* **2008**, *27* (39), 5182–5194.
- (53) Yang, J.; Price, M. A.; Li, G. Y.; Bar-Eli, M.; Salgia, R.; Jagadeeswaran, R.; Carlson, J. H.; Ferrone, S.; Turley, E. A.; McCarthy, J. B. Melanoma proteoglycan modifies gene expression to stimulate tumor cell motility, growth, and epithelial-to-mesenchymal transition. *Cancer Res.* **2009**, *69* (19), 7538–7547.

